1 **Title: "Carbon monoxide, a retrograde messenger generated in post-synaptic**
2 **mushroom body neurons evokes non-canonical dopamine release**."
3 Abbreviated title "Carbon monoxide evokes dopamine release"
4
5 Kohei Ueno[1]*, Johannes Morstein[2,3], Kyoko Ofusa[1], Shintaro Naganos[1], Ema
6 Suzuki-Sawano[1], Saika Minegishi[4], Samir P. Rezgui[5], Hiroaki Kitagishi[4], Brian W.
7 Michel[5], Christopher J. Chang[2], Junjiro Horiuchi[1], Minoru Saitoe[1]*
8
9 [1]Tokyo Metropolitan Institute of Medical Science, 2-1-6 Kamikitazawa, Setagaya-ku,
10 Tokyo, 1568506, Japan.
11 [2]Departments of Chemistry and Howard Hughes Medical Institute, University of
12 California, Berkeley, CA, 94720, USA.
13 [3]Department of Chemistry, New York University, NY 10012, USA.
14 [4]Department of Molecular Chemistry and Biochemistry, Faculty of Science and
15 Engineering, Doshisha University, Kyotanabe, Kyoto, 6100321, Japan.
16 [5]Department of Chemistry and Biochemistry, University of Denver, CO, 80208, USA.
17
18 *Correspondence to: Kohei Ueno (ueno-kh@igakuken.or.jp), and Minoru Saitoe
19 (saito-mn@igakuken.or.jp)
20
21 Keywords: Drosophila, dopamine, retgrade messenger, carbon monoxide
22 Number of pages: 55
23 Number of figures and table: 5 main figures
24 Number of words for abstract, introcution and discussion: 144 (abstract), 678

(introduction) and 2068 (discussion)

Conflict of interest statement; The authors declare that there is no conflict of interest.

ACKNOWLEDGMENTS

This work was supported by grants from the Japanese Society for the Promotion of Science (JP17K07122) to K.U., a Grant-in-Aid for Scientific Research in Innovative Areas “Memory dynamism” (JP25115006) to M.S., and NIH (GM79465) to C.J.C. C.J.C. is an Investigator with the Howard Hughes Medical Institute. We thank A. Nose for *UAS-R-GECO1* transgenic flies, and T. Miyashita, M. Matsuno, T. Ueno and Y. Hirano for helpful discussions. The authors declare no competing financial interests.

AUTHOR CONTRIBUTION

K.U. and M.S. designed the experiments. K.U. performed most imaging experiments with K.O., S.N., and E.S. CO scavenger was synthesized by S.M., and H.K. CO probe was synthesized by J.M., and C.J.C. The limit of detection of COP-1 is measured by S.P.R. and B.W.M. The manuscript was written by M.S. and J.H. with K.U.

ABSTRACT

Dopaminergic neurons innervate extensive areas of the brain and release dopamine (DA) onto a wide range of target neurons. However, DA release is also precisely regulated, and in *Drosophila*, DA is released specifically onto mushroom body (MB) neurons, which have been coincidentally activated by cholinergic and glutamatergic inputs. The mechanism for this precise release has been unclear. Here we found that coincidentally activated MB neurons generate carbon monoxide (CO) which functions as a retrograde signal evoking local DA release from presynaptic terminals. CO production depends on activity of heme oxygenase in post-synaptic MB neurons, and CO-evoked DA release requires Ca^{2+} efflux through ryanodine receptors in DA terminals. CO is only produced in MB areas receiving coincident activation, and removal of CO using scavengers blocks DA release. We propose that DA neurons utilize two distinct modes of transmission to produce global and local DA signaling.

SIGNIFICANCE STATEMENT

Dopamine (DA) is needed for various higher brain functions including memory formation. However, DA neurons form extensive synaptic connections, while memory formation requires highly specific and localized DA release. Here we identify a mechanism through which DA release from presynaptic terminals is controlled by postsynaptic activity. Postsynaptic neurons activated by cholinergic and glutamatergic inputs generate carbon monoxide, which acts as a retrograde messenger inducing presynaptic DA release. Released DA is required for memory-associated plasticity. Our

work identifies a novel mechanism that restricts DA release to the specific postsynaptic sites that require DA during memory formation.

INTRODUCTION

Dopamine (DA) is required for various brain functions including the regulation of global brain states such as arousal and moods(Huang and Kandel, 1995; Molina-Luna et al., 2009; Yagishita et al., 2014). To perform these functions, individual DA neurons innervate extensive areas of the brain and release DA onto a wide range of target neurons through a processes known as volume transmission(Agnati et al., 1995; Rice and Cragg, 2008; Matsuda et al., 2009). However, this extensive innervation is not suitable for precise, localized release of DA, and it has been unclear how widely innervating dopaminergic neurons can also direct DA-release onto specific target neurons.

In *Drosophila*, olfactory associative memories are formed and stored in the mushroom bodies (MBs) where Kenyon cells, MB intrinsic neurons which are activated by different odors, form synaptic connections with various MB output neurons (MBONs) which regulate approach and avoidance behaviors(Gerber et al., 2004; Aso et al., 2014). Dopaminergic neurons modulate plasticity of Kenyon cell MBON synapses(Claridge-Chang et al., 2009; Aso et al., 2010; Aso et al., 2012; Liu et al., 2012). However, while there are approximately 2000 to 2500 Kenyon cells that form thousands of synapses with MBONs, plasticity at these synapses is regulated by relatively few DA neurons(Mao and Davis, 2009). This indicates that canonical action potential-dependent release cannot fully explain DA release and plasticity. We recently determined that in *Drosophila*, synaptic vesicular (SV) exocytosis from DA terminals is restricted to

mushroom body (MB) neurons that have been activated by coincident inputs from odor-activated cholinergic pathways, and glutamatergic pathways, which convey somatosensory (pain) information(Ueno et al., 2017). Odor information is transmitted to the MB by projection neurons (PNs) from the antennal lobe (AL)(Marin et al., 2002; Wong et al., 2002), while somatosensory information is transmitted to the brain via ascending fibers of the ventral nerve cord (AFV). AL stimulation evokes Ca^{2+} responses in the MB by activating nicotinic acetylcholine receptors (nAChRs), and AFV stimulation evokes Ca^{2+} responses in the MBs by activating NMDA receptors (NRs) in the MBs(Ueno et al., 2013). Significantly, when the AL and AFV are stimulated simultaneously (AL + AFV) or the AL and NRs are stimulated simultaneously (AL + NMDA), plasticity occurs such that subsequent AL stimulations causes increased Ca^{2+} responses in the α3/α'3 compartments of the vertical MB lobes(Wang et al., 2008; Ueno et al., 2013). This plasticity is known as long-term enhancement (LTE) of MB responses and requires activation of D1 type DA receptors (D1Rs) in the MBs. Furthermore, while activation of D1Rs alone is sufficient to produce LTE, neither AL nor AFV stimulation alone is able to cause SV exocytosis from presynaptic DA terminals projecting onto the α3/α'3 compartments of the vertical MB lobes. Instead, exocytosis from DA terminals occurs only when postsynaptic Kenyon cells are activated by coincident AL + AFV or AL + NMDA stimulation. Strikingly, while MBs are bilateral structures and DA neurons project terminals onto both sides of MBs(Mao and Davis, 2009), SV exocytosis occurs specifically in MB areas that have been coincidently activated. Based on these results, we proposed that coincident inputs specify the location where DA is released, while DA induces plastic changes needed to encode associations. However, it has been unclear how activated Kenyon cells induce SV exocytosis from presynaptic DA terminals. Locally

115 restricted SV exocytosis upon coincident activation of Kenyon cells requires activity of
116 the *rutabaga* type of adenylyl cyclase, which is proposed to be a coincident detector in
117 the MBs. Thus Kenyon cells may sense coincident activation and send a retrograde
118 "demand" signal to presynaptic terminals to evoke local DA release(Ueno et al., 2017).
119 In this study, we used a *Drosophila* dissected brain system to examine synaptic
120 plasticity and DA release, and found that coincidentally activated post-synaptic Kenyon
121 cells generate the retrograde messenger, carbon monoxide (CO). CO is generated by
122 heme oxygenase (HO) in post-synaptic MB neurons, and induces DA release from
123 pre-synaptic terminals by evoking Ca^{2+} release from internal stores via ryanodine
124 receptors (RyRs). Thus, while individual DA neurons extensively innervate the MBs,
125 on-demand SV exocytosis allows DA neurons to induce plasticity in specific target
126 neurons.
127
128 **MATERIALS AND METHODS**
129 **Fly Stock maintenance**
130 All fly stocks were raised on standard cornmeal medium at 25 ± 2˚C and 60 ± 10%
131 humidity under a 12/12 h light–dark cycle. Flies were used for experiments 1-3 d after
132 eclosion.
133
134 **Transgenic and mutant lines**
135 All transgenic and mutant lines used in this study are listed in supplemental Table S1.
136 *UAS-G-CaMP3* (BDSC_32234, Bloomington Stock Center, Indiana), *LexAop-G-CaMP2*
137 (Ueno et al., 2013) and *LexAop-R-GECO1* lines were used for measuring Ca^{2+} responses
138 as described previously(Ueno et al., 2013). *UAS-synapto-pHluorin* (*UAS-spH*)(Ng et al.,

2002) and *LexAop-synapto-pHluorin* (*LexAop-spH*) lines were used for measuring vesicle release(Ueno et al., 2013). *MB-LexA::GAD* (Ueno et al., 2013) was used for the *LexA* MB driver, *c747* (Aso et al., 2009) was used as the *GAL4* MB driver, and (Friggi-Grelin et al., 2003) and *TH-LexAp65* (Ueno et al., 2013) were used for *TH-DA* drivers. *UAS-shi^{ts}* (Kitamoto, 2001) and *pJFRC104-13XLexAop2-IVS-Syn21-Shibire-ts1-p10* (*LexAop-shi^{ts}*)(Pfeiffer et al., 2012) lines were used for inhibition of synaptic transmission. *MB247-Switch* (*MBsw*) was to express a *UAS* transgene in the MBs upon RU486 (RU+) feeding for 3-5 days(Mao et al., 2004). *UAS-dHO IR* was used to knockdown of *dHO* expression(Cui et al., 2008). *dHO$^{\Delta}$* is a deficiency line *Df(3R)Exel7309* (BDSC 7960), lacking 65 Kbp including *dHO* (Flybase; http://flybase.org) in the third chromosome. *P{KK101716}VIE-260B* (VDRC ID 109631, Vienna Drosophila Resource Center, Vienna, Austria) (*UAS-RyR RNAi*) was used to knock down *RyR*. *Mi{Trojan-GAL4.0}RyR[MI08146-TG4.0]* (BDSC 67480) carries a *GAL4* sequence between 18 and 19 exon of *RyR* and was used to monitor *RyR* gene expression.

Isolated whole brain preparation

Brains were prepared for imaging as previously described(Ueno et al., 2013). Briefly, brains were dissected in ice cold 0 mM Ca^{2+} HL3 medium (in mM, NaCl, 70; sucrose, 115; KCl, 5; $MgCl_2$, 20; $NaHCO_3$, 10; trehalose, 5; Hepes, 5; pH 7.3 and 359 mOsm)(Stewart et al., 1994), and placed in a recording chamber filled with normal, room temperature HL3 medium (the same recipe as above, containing 1.8 mM $CaCl_2$). To deliver hemoCD through the blood brain barrier, brains were treated with papain (10 U/ml) for 15 min at room temperature, and washed several times with 0 mM Ca^{2+} HL3

163 medium prior to use(Gu and O'Dowd, 2007; Ueno et al., 2017).

164

165 **Imaging analysis**

166 Imaging analysis was performed in HL3 solution as described previously (Ueno et al.,
167 2013; Ueno et al., 2017). Briefly, fluorescent images were captured at 15 Hz using a
168 confocal microscope system (A1R, Nikon Corp., Tokyo, Japan) with a 20x
169 water-immersion lens (numerical aperture 0.5; Nikon Corp). We obtained F_0 by
170 averaging the 5 sequential frames before stimulus onset and calculated $\Delta F/F_0$. To
171 evaluate stimulation-induced fluorescent changes of spH, $\Delta F/F_0$ calculated in the
172 absence of stimulation or pharmacological agents was subtracted from stimulus or drug
173 induced $\Delta F/F_0$. To quantitatively evaluate the spH fluorescent changes, the average
174 values of fluorescent changes at indicated time points during and after stimulation were
175 statistically compared.

176 The AL was stimulated (30 pulses, 100 Hz, 1.0 ms pulse duration) using glass
177 micro-electrodes. For NMDA stimulation, 200 μM NMDA, diluted in HL3 containing 4
178 mM Mg^{2+} (Miyashita et al., 2012), was applied by micro pipette.

179 For application of CO-saturated HL3, CO or control N_2 gas was dissolved in HL3
180 saline by bubbling. CO or N_2 saturated solutions were immediately placed in glass
181 pipettes and puffed onto the MB lobes for 1 min (pressure = 6 psi) using a Picospritzer
182 III system (Parker Hannifin Corp., USA). While we first used thin tip micropipettes,
183 approximately 5 micro m diameter (Fig. 2*A*), we also used larger tip micropipettes,
184 approximately 15 micro m (Fig. 5*E*), to avoid clogging.

185 To measure SV exocytosis using FFN511, *MB-LexA:GAD, LexAop-R-GECO1* brains
186 were incubated in 10 μM FFN511/HL3 for 30 min. To remove non-specific binding of

187 the dye, FFN511 loaded brains were washed in 200 μM ADVASEP-7/HL3 for 15 min
188 two times(Kay et al., 1999; Gubernator et al., 2009). To evaluate stimulation-induced
189 release of FFN511, $\Delta F/F_0$ in the absence of stimulation was subtracted from $\Delta F/F_0$
190
191 **Behaviors**
192 Olfactory aversive memory: The procedure for measuring olfactory memory has been
193 previously described(Tully and Quinn, 1985; Tamura et al., 2003). Briefly, two mildly
194 aversive odors (3-octanol [OCT]) or 4-methylcyclohexanol [MCH]) were sequentially
195 delivered to approximately 100 flies for 1 min with a 45 sec interval between each odor
196 presentation. When flies were exposed to the first, CS^+ odor (either OCT or MCH), they
197 were also subjected to 1.5 sec pulses of 60 V DC electric shocks every five sec. To test
198 olfactory memory, flies were placed at the choice point of a T-maze where they were
199 allowed to choose either the CS+ or CS- odor for 1.5 min. Memory was calculated as a
200 performance index (PI), such that a 50:50 distribution (no memory) yielded a
201 performance index of zero and a 0:100 distribution away from the CS^+ yielded a
202 performance index of 100.
203
204 Odor and Shock avoidance. Peripheral control experiments including odor and shock
205 reactivity assays were performed as previously described(Tully and Quinn, 1985) to
206 measure sensitivity to odors and electrical shocks. Approximately 100 flies were placed
207 at the choice point of a T maze where they had to choose between an odor (OCT or
208 MCH) and mineral oil or between electrical shocks and non-shocked conditions. A
209 preformance index was calculated as described above.
210

211 **Identification of dHO localization**

212 To detect of dHO protein in fly brains, wild-type, w(CS)(Dura et al., 1993), and *dHO*$^{\Delta}$
213 flies were dissected and fixed in 4 % paraformaldehyde for 20 min at 4°C. Brains were
214 incubated in PBS with 5 % FBS and 0.1 % Triton-X for 30 min at 4°C, and then in
215 primary antibodies, 1:50 anti-HO (Cui et al., 2008) and 1:20 anti-Fas2 (1D4,
216 Developmental Studies Hybridoma Bank, Iowa, USA) for 3 days at 4°C. After washing,
217 brains were incubated with secondary antibodies, Alexa488-conjugated donkey anti-rat
218 antibody (1:200) (Invitrogen, Carlsbad, USA) and Alexa555-conjugated donkey
219 anti-mouse antibody (1:200) (Invitrogen) for 2 days at 4°C. Images were captured using
220 an A1R confocal microscope (Nikon, Tokyo, Japan).

221

222 **Identification of RyR positive neurons (Trojan)**

223 For *Mi{Trojan-GAL4.0}RyR[MI08146-TG4.0]/UAS-mCD8::GFP* imaging, heads were
224 dissected in 4 % paraformaldehyde for 30 min at 4°C. Brains were incubated with
225 primary antibodies, anti-GFP (1:400) (ab13970, Abcam, Cambridge, UK) and
226 anti-tyrosine hydroxylase (#22941, Immunostar, Hudson, USA) in PBS with 10 %
227 ImmunoBlock (DS Pharma Biomedical Co., Osaka, Japan) and 0.1 % Triton-X
228 overnight at 4°C. After washing, brains were incubated with secondary antibodies,
229 Alexa488-conjugated donkey anti-chick antibody (1:400) (Jackson ImmunoResearch,
230 West Grove, USA) and Alexa555-conjugated donkey anti-mouse antibody (1:400)
231 (Invitrogen) overnight at 4°C. Images were captured using an A1R confocal microscope
232 (Nikon, Tokyo, Japan).

233

234 **Chemicals and treatments**

RU486 (mifepristone), NMDA (N-methyl-D-aspartate), L-NAME (Nϖ-L-nitro arginine methyl ester), 1-octanol, 2-arachidonil glycerol, arachidonic acid and CrMP (chromium mesoporphyrin) and ADVASEP-7 were purchased from Sigma-Aldrich (Missouri, USA). Thapsigargin and tetrodotoxin (TTX) were purchased from Wako Pure Chemical Industries (Osaka, Japan). Dantrolen was purchased from Alomone labs (Jerusalem, Israel). BAPTA-AM and O,O'-Bis(2-aminoethyl)ethyleneglycol-N,N,N',N'-tetraacetic acid (EGTA) were purchased from Dojindo lab (Kumamoto, Japan). FFN511 was purchased from Abcam (Cambridge, England). Papain was purchased from Worthington Biochemical Corporation (New Jersey, USA). RU486 was dissolved in ethanol, butaclamol was dissolved in DMSO, L-NAME and SCH23390 were dissolved in water, CrMP was dissolved in 0.5% 2-aminoethanol and 2 mM HCl. Oxy-hemoCD was reduced in sodium dithionite and purified using a HiTrap Desalting column (GE Healthcare Japan, Tokyo, Japan) and eluted in PBS. The concentration of purified oxy-hemoCD is estimated by absorbance at 422 nm(Kitagishi et al., 2010). COP-1 and CORM-3 were prepared according to previous publications(Clark et al., 2003; Michel et al., 2012). Both reagents were stored at -20 °C and dissolved in DMSO before use. For RU486 treatment, dissolved RU486 was mixed in fly food. Flies were fed RU486 for 5 days prior to brain preparation. Other chemicals were treated as described in the main text and figure legends.

Statistics

Statistical analyses were performed using Prism software (GraphPad Software, Inc., La Jolla, CA, USA). All data in bar and line graphs are expressed as means ± SEMs. Student's t-test and Mann Whitney test was used to evaluate the statistical significance

between two data sets. For multiple comparisons, one-way or two-way ANOVA followed by Bonferroni post hoc analyses were employed. Statistical significances are shown as *P < 0.05, **P < 0.01. P values greater than 0.05 were considered not statistically significant, NS > 0.05.

RESULTS

CO synthesis in the MB neurons is required for DA release upon coincident stimulation

Previously, we used an *ex vivo* dissected brain system to examine SV exocytosis from DA terminals projecting onto the α3/α'3 compartments of the vertical MB lobes. We measured SV exocytosis from DA terminals using a vesicular exocytosis sensor, synapto-pHluorin (spH)(Miesenbock et al., 1998), expressed in dopaminergic neurons using a tyrosine hydroxylase (TH) driver, and found that release occurred only upon coincident activation of post-synaptic MB neurons by cholinergic inputs from the ALs and glutamatergic inputs from the AFV(Ueno et al., 2017).

If postsynaptic MB activity evokes SV exocytosis from presynaptic DA terminals, vesicular output from MB neurons may be needed to activate DA neurons that loop back to the MBs, as has been previously suggested(Ichinose et al., 2015; Cervantes-Sandoval et al., 2017; Takemura et al., 2017; Horiuchi, 2019). To test this possibility, we inhibited synaptic transmission from MB neurons by expressing temperature-sensitive shi^{ts} from a pan-MB driver, *MB-LexA*. We confirmed that MB synaptic output is blocked at restrictive temperature in *MB-LexA>LexAop-*shi^{ts} flies by demonstrating that memory recall, which requires MB output(Dubnau et al., 2001;

283 McGuire et al., 2001), is defective in these flies (Suppelemental Fig. S1*A*).
284 Interestingly, SV exocytosis from TH-DA terminals occurs normally at restrictive
285 temperature in these flies upon coincident AL + NMDA stimulation (Fig. 1*A*),
286 suggesting while looping activity may be necessary for memory, it is not required for
287 DA release. SV exocytosis from TH-DA terminals also occurred normally when *shi*^{ts}
288 was expressed using a different MB driver (*c747-GAL4>UAS-shi*^{ts}) (Suppelemental Fig.
289 S1*B*), even though memory recall was also disrupted at restrictive temperature in this
290 line(Dubnau et al., 2001). 1 mM 1-octanol, a blocker of gap junctional
291 communication(Rorig et al., 1996; Goncharenko et al., 2014), also did not inhibit SV
292 exocytosis in TH-DA terminals (Fig. 1*B*). These results suggest that output from
293 chemical and electrical synapses is not required for post-synaptic MB neurons to induce
294 pre-synaptic DA-release from DA neurons.

295 We next examined whether a retrograde messenger, such as nitric oxide (NO), may
296 be released from MB neurons to regulate pre-synaptic DA release. However, 100 μM
297 L-NAME (Nϖ-L-nitro arginine methyl ester), a NO synthetase blocker(Boultadakis and
298 Pitsikas, 2010) had no effect on AL + NMDA stimulation-induced SV exocytosis from
299 TH-DA terminals (Fig. 1*C*).

300 Olfactory memory is disrupted by mutations in *nemy*, a gene that encodes a
301 *Drosophila* homolog of cytochrome B561 (CytB561)(Iliadi et al., 2008), which is
302 involved in metabolism of carbon monoxide (CO)(Sugimura et al., 1980; Cypionka and
303 Meyer, 1983; Jacobitz and Meyer, 1989), a diffusible gas similar to NO, that also been
304 proposed to act as a retrograde messenger during synaptic plasticity(Alkadhi et al.,
305 2001; Shibuki et al., 2001). Thus, we next examined whether CO may be required for
306 DA release. CO is synthesized by heme oxygenase (HO), and we found that exocytosis

from TH-DA terminals upon coincident activation of MB neurons is abolished upon application of chromium mesoporphyrin (CrMP), a HO blocker(Vreman et al., 1993) (Fig. 1*D*). LTE was also significantly inhibited by CrMP (Suppelemental Fig. S2*A*), demonstrating the importance of DA release in plasticity. To verify that the *Drosophila* homologue of HO (dHO)(Cui et al., 2008) is present in the MBs, we used anti-dHO antibodies and found strong expression in the MBs and in insulin producing cells (Suppelemental Fig. S2*B*). We next inhibited *dHO* expression in the MBs using *MBsw>UAS-dHO-IR* flies, which express a *dHO-RNAi* construct from an RU486-inducible *MB247-switch* (*MBsw*) driver(Mao et al., 2004). We found that both SV exocytosis from TH-DA terminals (Fig. 1*E* and Suppelemental Movie S1*A, B*) as well as LTE (Suppelemental Fig. S2*C*) were impaired when these flies were fed RU486. Furthermore, acute knock down of dHO in the MBs in *MBsw>UAS-dHO-IR* flies disrupted olfactory memory (Suppelemental Fig. S2*D*) without affecting task-related responses (Suppelemental Fig. S2*E*). Altogether, these results indicate that dHO in the MBs is required for olfactory memory, MB plasticity, and DA release onto MBs.

CO generated from coincidentally activated MB neurons evokes DA release

If CO functions as a retrograde messenger inducing DA release, direct application of CO to DA terminals should induce release. Thus we next applied CO-saturated saline from micropipettes to the vertical lobes of the MBs, and observed robust SV exocytosis from TH-DA terminals (Fig. 2*B* and Suppelemental Movie S2). Further, we found that application of a CO-releasing molecule-3 (CORM-3), a water-soluble CO-donor(Tinajero-Trejo et al., 2014; Aki et al., 2018), also evokes SV exocytosis from TH-DA terminals (Fig. 2*B*). In contrast, application of other retrograde messengers,

331 including 200 μM arachidonic acid and 200 μM 2-arachidonylglycerol, an
332 endocanabinoid receptor agonist, had no effects on release (Fig. 2*C* and 2*D*). To further
333 examine whether endogenously generated CO is required for DA release, we used a CO
334 selective scavenger, hemoCD(Kitagishi et al., 2010) and found that hemoCD
335 significantly inhibited vesicular exocytosis from TH-DA terminals upon AL + NMDA
336 stimulation (Fig. 2*E*).

337 We next visualized the generation and release of CO from MB neurons using a CO
338 selective fluorescent probe, CO Probe 1 (COP-1)(Michel et al., 2012). While COP-1
339 fluorescence increased immediately after coincident AL + NMDA stimulation,
340 fluorescence remained unchanged after AL stimulation or NMDA application alone
341 (Fig. 3*A*). Thus, changes in COP-1 fluorescence parallel changes in DA release.
342 Furthermore, the fluorescence increase in COP-1 occurred on the lobes of the MBs
343 ipsilateral, but not contralateral, to the stimulated AL (Fig. 3*B* and Suppelemental
344 Movie S3). Since each AL innervates its ipsilateral, but not contralateral MB, this
345 suggests that CO production occurs in areas of coincident AL and NMDA activation.
346 Again this result parallels that of DA release(Ueno et al., 2017). Significantly, increased
347 COP-1 fluorescence was attenuated by knocking down dHO in the MBs (Fig. 3*C*),
348 indicating that COP-1 flurorescence detects dHO-dependent CO production.
349 Collectively, these results suggest that coincident stimulation of MB neurons induces
350 dHO to generate the retrograde messenger, CO, which then evokes SV exocytosis from
351 presynaptic DA terminals.

352

353 **CO evokes non-canonical SV exocytosis**

354 SV exocytosis requires an increase in Ca^{2+} concentration in presynaptic terminals(Katz

and Miledi, 1967; Augustine et al., 1985; Sabatini and Regehr, 1996; Meinrenken et al., 2003). Consistent with this, we observed a robust Ca^{2+} increase in TH-DA terminals that project onto the MB lobes receiving coincident AL + NMDA stimulation (Fig. 4*A* and Suppelemental Movie S4), but not in terminals that project to the contralateral side (Fig. 4*B*). Ca^{2+} increases in DA terminals were also observed upon application of CORM-3 (Fig. 4*C*), and this increase was abolished by addition of the membrane-permeable Ca^{2+} chelator BAPTA-AM (Fig. 4*D*). In canonical SV exocytosis, neuronal activity opens voltage-gated calcium channels, allowing influx of extracellular Ca^{2+}(Katz and Miledi, 1967; Augustine et al., 1985). However, we found that CORM-3 is able to induce SV exocytosis from TH-DA terminals even in Ca^{2+} free saline in the presence of the Ca^{2+} chelator, EGTA, and the sodium channel blocker, TTX (Fig. 4*E*). This suggests that CO-evoked DA release is action potential independent and does not require Ca^{2+} influx from extracellular sources.

Since extracellular Ca^{2+} is not responsible for CO-dependent DA release, we next examined whether Ca^{2+} efflux from internal stores may be required. Significantly, CORM-3 failed to increase Ca^{2+} in TH-DA terminals in the presence of EGTA and thapsigargin, an inhibitor of the sarcoplasmic/endoplasmic reticulum Ca^{2+} ATPase (SERCA), which depletes internal Ca^{2+} stores(Kijima et al., 1991; Sagara and Inesi, 1991) (Fig. 4*F*). Thus, CO-evoked DA release occurs through a non-canonical mechanism that depends on Ca^{2+} efflux from internal stores rather than from extracellular sources.

Ryanodine receptors mediate Ca^{2+} efflux for CO-evoked DA release.

What mediates Ca^{2+} efflux from internal stores in DA terminals? Inositol

1,4,5-trisphosphate receptors (IP_3Rs) and ryanodine receptors (RyRs) are the major channels mediating Ca^{2+} release from internal stores(Bardo et al., 2006). While SV exocytosis evoked by coincident MB stimulation was not suppressed by 2-Aminoethoxydiphenyl borate (2-APB), an IP_3R antagonist(Maruyama et al., 1997) (Fig. 5*A*), exocytosis was significantly inhibited by dantrolene, a RyR antagonist(Zhao et al., 2001) (Fig. 5*B*). Conversely, application of a RyR agonist, 4-chloro-3-methylphenol (4C3MP)(Zorzato et al., 1993) was sufficient to evoke exocytosis (Fig. 5*C*). These data suggest that RyRs in DA neurons are required for SV exocytosis upon coincident activation of MB neurons.

To address whether RyRs are expressed in DA terminals, we examined expression of mCD8::GFP in *Mi{Trojan-GAL4.0}RyR*$^{MI08146\text{-}TG4.0}$*; P{UAS-mCD8::GFP}* flies. In *Mi{Trojan-GAL4.0}RyR*$^{MI08146\text{-}TG4.0}$, a Trojan GAL4 exon is inserted between exons 18 and 19 in the same orientation as the RyR gene(Diao et al., 2015). Thus GAL4, and mCD8::GFP, expression should reflect RyR expression. In these flies, mCD8::GFP signals overlapped with anti-TH antibody signals, indicating that RyRs are expressed in DA neurons (Suppelemental Fig. 3*A*). To determine whether RyRs in the DA terminals are required for DA release, we used the TARGET system(McGuire et al., 2003) to acutely knock down RyRs in adult TH-DA neurons, and found that this significantly suppressed SV exocytosis from DA terminals upon AL + NMDA stimulation (Fig. 5*D*). Furthermore, acute knock down RyRs also suppressed SV exocytosis induced by direct CO application to TH-DA terminals (Fig. 5*E*), and also suppressed LTE upon coincident AL + NMDA stimulation (Suppelemental Fig. S3*B*). Thus, pre-synaptic RyRs are required for both activation-dependent and CO-dependent DA release, MB plasticity, and olfactory memory.

DISCUSSION

CO functions as a retrograde on-demand messenger for SV exocytosis in presynaptic DA terminals

A central tenet of neurobiology is that action potentials, propagating from the cell bodies, induce Ca^{2+} influx in presynaptic terminals to evoke SV exocytosis. However, recent mammalian studies have shown that only a certain fraction of a large number of pre-synaptic release sites is involved in canonical SV exocytosis(Pereira et al., 2016; Liu et al., 2018). In this study we identify a novel mechanism of SV exocytosis in which activity in post-synaptic neurons evokes pre-synaptic release to induce plastic changes. This mechanism allows the timing and location of DA release to be strictly defined by activity of postsynaptic neurons.

On-demand SV exocytosis utilizes CO as a retrograde signal from postsynaptic MB neurons to presynaptic DA terminals. We demonstrate that CO fulfills the criteria that have been proposed for a retrograde messenger(Regehr et al., 2009). First, we demonstrate that HO, which catalyzes CO production, is highly expressed in postsynaptic MB neurons, indicating that MB neurons have the capacity to synthesize the messenger. Second, we show that pharmacological and genetic suppression of HO activity in the MBs inhibits CO production, pre-synaptic DA release, and LTE. Third, using a CO fluorescent probe, COP-1(Michel et al., 2012), we demonstrate that CO is generated in the MBs following coincident stimulation of the MBs, and CO generation is restricted to lobes of MB neurons that receive coincident stimulation. We further show that direct application of CO, or a CO donor, induces DA release from presynaptic terminals, while

addition of a CO scavenger, HemoCD, suppresses release. Fourth, we demonstrate that CO activates RyRs in presynaptic terminals to induce SV exocytosis. Strikingly, CO-dependent SV exocytosis does not depend on influx of extracellular Ca^{2+}, but instead requires efflux of Ca^{2+} from internal stores via RyRs. Finally, we show that pharmacological inhibition and genetic suppression of RyRs in DA neurons impairs DA release after coincident stimulation and CO application.

Other retrograde signals, such as NO and endo cannabinoids enhance or suppress canonical SV exocytosis, we find that CO-dependent DA release occurs even in conditions which block neuronal activity and Ca^{2+} influx in presynaptic DA terminals. This suggests that CO does not function to modulate canonical SV exocytosis, but may instead evoke exocytosis through a novel mechanism. Several previous studies have indicated that CO and RyR-dependent DA release also occurs in mammals. A microdialysis study has shown that CO increases the extracellular DA concentration in the rat striatum and hippocampus(Hiramatsu et al., 1994), either through increased DA release, or inhibition of DA reuptake(Taskiran et al., 2003). Also, pharmacological stimulation of RyRs has been reported to induce DA release in the mice striatum(Oyamada et al., 1998; Wan et al., 1999). This release is attenuated in RyR3 deficient mice, while KCl-induced DA release, which requires influx of extracellular Ca^{2+}, is unaffected, suggesting that RyR-dependent release is distinct from canonical DA release. However, it has been unknown whether and how CO is generated endogenously. Also physiological conditions that activate RyRs to evoke DA release have also been unclear.

While our results demonstrate that CO signaling is necessary and sufficient for DA release, we note that our studies use fluorescent reporters which are not optimal for

detailed kinetic analysis of release and reuptake. For example, increases in spH fluorescence can be used to determine vesicular release from DA neurons, but the decrease in spH fluorescence after release does not reflect the kinetics of clearance of DA from synaptic sites. Similarly, increases in COP-1 fluorescence reflect increases in CO production and release, but the kinetics of this increase depends on CO binding affinities and limit of detection (Suppelemental Fig. S4) as well as CO production, and the gradual increase in COP-1 fluorescence following coincident activation does not indicate that CO production is similarly gradual. In addition, since COP-1 binding to CO is irreversible, we do not see a decrease in COP-1 fluorescence after the end of stimulation. Thus, although our functional imaging studies reliably measure significant changes in synaptic release, calcium signaling, and CO production, they are not precise enough to accurately measure the fast dynamics of these changes.

Signaling pathway for CO-dependent on-demand release of DA

While most neurotransmitters are stored in synaptic vesicles and released upon neuronal depolarization, the release of gaseous retrograde messengers such as NO and CO is likely coupled to activation of their biosynthetic enzymes, NOS and HO. Previously, we demonstrated that activity-dependent DA release onto the MBs requires *rutabaga* adenylyl cyclase (*rut*-AC) in the MBs(Ueno et al., 2017). *rut*-AC is proposed to function as a neuronal coincidence detector that senses coincident sensory inputs and activates the PKA pathway by increasing production of cAMP. In mammals, activation of the cAMP/PKA pathway increases expression of an HO isoform, HO-1, through transcriptional activation of the transcription factor CREB(Durante et al., 1997; Park et al., 2013; Astort et al., 2016). However, gene expression changes are not fast enough to

475 explain CO-dependent DA release. A second mammalian HO isoform, HO-2 is
476 selectively enriched in neurons, and HO-2-derived CO is reported to function in plasticity.
477 HO-2 is activated by Ca^{2+}/calmodulin (CaM) binding(Boehning et al., 2004), and by
478 casein kinase II (CKII) phosphorylation(Boehning et al., 2003), two mechanisms that can
479 generate CO with sufficient speed to account for LTE. Currently, it is unclear whether
480 *rut*-AC and the cAMP/PKA pathway functions in parallel with Ca^{2+}/CaM and CKII, or in
481 concert with these pathways (ie functions as a priming kinase for CKII(Huang et al.,
482 2007)) to activate HO. Supporting the concept that PKA regulates HO, in the golden
483 hamster retina, PKA has been shown to increase HO activity without affecting HO gene
484 expression(Sacca et al., 2003).

485 While *Drosophila* has a single isoform of RyR, mammals have three isoforms, RyR1
486 to RyR3. Skeletal muscle and cardiac muscle primarily express RyR1 and RyR2, and the
487 brain, including the striatum, hippocampus and cortex, expresses all three
488 isoforms(Giannini et al., 1995). RyRs are known to be activated by Ca^{2+} to mediate Ca^{2+}
489 induced Ca^{2+} release (CICR)(Endo, 2009). However, CO-evoked DA release occurs even
490 in the presence of Ca^{2+}-free extracellular solutions containing TTX and EGTA,
491 suggesting that CO activates RyRs through a different mechanism. Besides Ca^{2+}, RyRs
492 can be activated by calmodulin, ATP, PKA, PKG, cADP-ribose, and NO(Takasago et al.,
493 1991; Xu et al., 1998; Verkhratsky, 2005; Zalk et al., 2007; Lanner et al., 2010; Kakizawa,
494 2013). NO can directly stimulate RyR1 non-enzymatically by S-nitrosylating a histidine
495 residue to induce Ca^{2+} efflux(Xu et al., 1998; Kakizawa, 2013). Similarly, CO has been
496 reported to activate Ca^{2+}-activated potassium channels (K_{Ca}) through a non-enzymatic
497 reaction in rat artery smooth muscle(Wang and Wu, 2003). Alternatively, both NO and
498 CO can bind to the heme moiety of soluble guanylate cyclase (sGC) leading to its

activation(Stone and Marletta, 1994). Activated sGC produces cGMP, and cGMP-dependent protein kinase (PKG) rapidly phosphorylates and activates RyRs(Takasago et al., 1991). Interestingly, NO increases DA in the mammalian striatum in a neural activity independent manner(Hanbauer et al., 1992; Zhu and Luo, 1992; Lonart et al., 1993). Since activation of RyRs also increases extracellular DA in the striatum, hippocampus and cortex(Oyamada et al., 1998; Wan et al., 1999), NO may play a pivotal role in RyR activation and DA release in mammals. However, NOS expression has not been detected in the MBs(Muller, 1994; Regulski and Tully, 1995), suggesting that in *Drosophila*, CO rather than NO may function in this process.

Biological significance of on-demand DA release

DA plays a critical role in associative learning and synaptic plasticity(Huang and Kandel, 1995; Jay, 2003; Puig et al., 2014; Lee et al., 2016; Yamasaki and Takeuchi, 2017). In flies, neutral odors induce MB responses by activating sparse subsets of MB neurons. After being paired with electrical shocks during aversive olfactory conditioning, odors induce larger MB responses in certain areas of the MBs(Yu et al., 2006; Wang et al., 2008; Akalal et al., 2011; Davis, 2011). We modeled this plastic change in *ex vivo* brains as LTE, and showed that DA application alone is sufficient to induce this larger response(Ueno et al., 2017). However, in the *Drosophila* brain, only a small number of DA neurons (~12 for aversive and ~100 for appetitive) regulate plasticity in ~2000 MB Kenyon cells(Mao and Davis, 2009). Thus to form odor-specific associations, there should be a mechanism regulating release at individual synapses. CO-dependent on-demand DA release provides this type of control. If on-demand release is involved in plasticity and associative learning, knockdown of genes associated with release should affect learning. Indeed, we show that

523 knocking down either dHO in the MBs or RyRs in DA neurons impairs olfactory
524 conditioning. While these knockdowns did not completely abolish olfactory conditioning,
525 this may be due to inefficiency of our knockdown lines. Alternatively, on-demand release
526 may not be the only mechanism responsible for memory formation, but may instead be
527 required for a specific phase of olfactory memory.

528 In olfactory aversive conditioning, CS+ odor is paired with US electrical shock.
529 Given that AFV conveys US information, it seems strange that DA is not released by
530 AFV stimulation alone in our *ex vivo* imging, while previous *in vivo* imaging study
531 demonstrated that DA is released by electrical shock presentation alone (Sun et al.,
532 2018). Notably, projection of DA terminals are compartmentalized on the MB lobes and
533 show distinct responses and DA release during sensory processing (Cohn et al., 2015;
534 Sun et al., 2018). In our *ex vivo* imaging, we looked at DA release onto the α3/α'3
535 compartments of the MB vertical lobes, while the previous *in vivo* imaging study found
536 DA release onto the γ2 and γ3 compartments of the MB horizontal lobes upon electrical
537 shock (Sun et al., 2018). Therefore, AFV stimulation may also induce DA release onto
538 these horizontal compartments although it does not induce DA release onto α3/α'3
539 compartments. However, due the location of the microelectrode for AL stimulation, we
540 did not look at the horizontal lobes in this study. Another possibility is that arousal state
541 of the flies in *in vivo imaging* may be essential for DA release upon shock presentation.
542 While our *ex vivo* imaging study supposes that glutamatergic neurons transmit AFV
543 information to the MBs (Ueno et al., 2017), aversive US information has been proposed
544 to be transmitted by DA neurons (Claridge-Chang et al., 2009; Aso et al., 2010; Aso et
545 al., 2012; Burke et al., 2012; Liu et al., 2012). Synaptic terminals immunoreactive for
546 the vesicular glutamate transporter, VGLUT, have been identified at the α3

compartment of the MB vertical lobes (Daniels et al., 2008). However, recent connectome study demonstrates that they are presynaptic terminals of the MB output neurons (Takemura et al., 2017). Nevertheless, it is noteworthy that these immunohisitochemical and connectome data do not correlate with expression of NMDA receptors in the MBs (Miyashita et al., 2012). These mismatch observations implicate that AFV mediated shock information may be transmitted to the MBs by another type of glutamatergic neurons.

In mammals, the role of CO in synaptic plasticity is unclear. Application of CO paired with low frequency stimulation induces LTP, while inhibiting HO blocks LTP in the CA1 region of the hippocampus(Zhuo et al., 1993). However, HO-2 deficient mice have been reported to have normal hippocampal CA1 LTP(Poss et al., 1995). In contrast to CO, a role for NO in synaptic plasticity and learning has been previously reported(Muller, 1996; Balaban et al., 2014; Korshunova and Balaban, 2014). Thus, at this point it is an open question whether CO or NO evokes DA release in mammals. Downstream from CO or NO, RyRs have been shown to be required for hippocampal and cerebellum synaptic plasticity(Wang et al., 1996; Balschun et al., 1999; Lu and Hawkins, 2002; Kakizawa et al., 2012).

Our current results suggest that DA neurons release DA via two distinct mechanisms: canonical exocytosis and on-demand release. Canonical exocytosis is evoked by electrical activity of presynaptic DA neurons, requires Ca^{2+} influx, and may be involved in volume transmission. This mode of release can activate widespread targets over time, and is suited for regulating global brain functions. In contrast, on-demand release is evoked by activity of postsynaptic neurons, requires Ca^{2+} efflux via RyRs, and can regulate function of specific targets at precise times. DA neurons may differentially

utilize these two modes of SV exocytosis in a context dependent manner. Understanding how DA neurons differentially utilize these modes of transmission will provide new insights into how a relatively small number of DA neurons can control numerous different brain functions.

577 **REFERENCES**

578 Agnati LF, Zoli M, Stromberg I, Fuxe K (1995) Intercellular communication in the
579 brain: wiring versus volume transmission. Neuroscience 69:711-726.

580 Akalal DB, Yu D, Davis RL (2011) The long-term memory trace formed in the
581 Drosophila alpha/beta mushroom body neurons is abolished in long-term
582 memory mutants. The Journal of neuroscience : the official journal of the
583 Society for Neuroscience 31:5643-5647.

584 Aki T, Unuma K, Noritake K, Kurahashi H, Funakoshi T, Uemura K (2018) Interaction
585 of carbon monoxide-releasing ruthenium carbonyl CORM-3 with plasma
586 fibronectin. Toxicol In Vitro 50:201-209.

587 Alkadhi KA, Al-Hijailan RS, Malik K, Hogan YH (2001) Retrograde carbon monoxide
588 is required for induction of long-term potentiation in rat superior cervical
589 ganglion. The Journal of neuroscience : the official journal of the Society for
590 Neuroscience 21:3515-3520.

591 Aso Y, Grubel K, Busch S, Friedrich AB, Siwanowicz I, Tanimoto H (2009) The
592 mushroom body of adult Drosophila characterized by GAL4 drivers. J
593 Neurogenet 23:156-172.

594 Aso Y, Siwanowicz I, Bracker L, Ito K, Kitamoto T, Tanimoto H (2010) Specific
595 dopaminergic neurons for the formation of labile aversive memory. Curr Biol
596 20:1445-1451.

597 Aso Y, Herb A, Ogueta M, Siwanowicz I, Templier T, Friedrich AB, Ito K, Scholz H,
598 Tanimoto H (2012) Three dopamine pathways induce aversive odor memories
599 with different stability. PLoS genetics 8:e1002768.

600 Aso Y et al. (2014) Mushroom body output neurons encode valence and guide
601 memory-based action selection in Drosophila. Elife 3:e04580.

602 Astort F, Repetto EM, Rocha-Viegas L, Mercau ME, Puch SS, Finkielstein CV, Pecci A,
603 Cymeryng CB (2016) Role of CREB on heme oxygenase-1 induction in adrenal

604 cells: involvement of the PI3K pathway. J Mol Endocrinol 57:113-124.

605 Augustine GJ, Charlton MP, Smith SJ (1985) Calcium entry and transmitter release at
606 voltage-clamped nerve terminals of squid. The Journal of physiology
607 367:163-181.

608 Balaban PM, Roshchin M, Timoshenko AK, Gainutdinov KL, Bogodvid TK, Muranova
609 LN, Zuzina AB, Korshunova TA (2014) Nitric oxide is necessary for labilization
610 of a consolidated context memory during reconsolidation in terrestrial snails.
611 The European journal of neuroscience 40:2963-2970.

612 Balschun D, Wolfer DP, Bertocchini F, Barone V, Conti A, Zuschratter W, Missiaen L,
613 Lipp HP, Frey JU, Sorrentino V (1999) Deletion of the ryanodine receptor type 3
614 (RyR3) impairs forms of synaptic plasticity and spatial learning. EMBO J
615 18:5264-5273.

616 Bardo S, Cavazzini MG, Emptage N (2006) The role of the endoplasmic reticulum
617 Ca2+ store in the plasticity of central neurons. Trends Pharmacol Sci 27:78-84.

618 Boehning D, Sedaghat L, Sedlak TW, Snyder SH (2004) Heme oxygenase-2 is activated
619 by calcium-calmodulin. J Biol Chem 279:30927-30930.

620 Boehning D, Moon C, Sharma S, Hurt KJ, Hester LD, Ronnett GV, Shugar D, Snyder
621 SH (2003) Carbon monoxide neurotransmission activated by CK2
622 phosphorylation of heme oxygenase-2. Neuron 40:129-137.

623 Boultadakis A, Pitsikas N (2010) Effects of the nitric oxide synthase inhibitor L-NAME
624 on recognition and spatial memory deficits produced by different NMDA
625 receptor antagonists in the rat. Neuropsychopharmacology : official publication
626 of the American College of Neuropsychopharmacology 35:2357-2366.

627 Burke CJ, Huetteroth W, Owald D, Perisse E, Krashes MJ, Das G, Gohl D, Silies M,
628 Certel S, Waddell S (2012) Layered reward signalling through octopamine and
629 dopamine in Drosophila. Nature 492:433-437.

630 Cervantes-Sandoval I, Phan A, Chakraborty M, Davis RL (2017) Reciprocal synapses

631 between mushroom body and dopamine neurons form a positive feedback loop
632 required for learning. Elife 6.

633 Claridge-Chang A, Roorda RD, Vrontou E, Sjulson L, Li H, Hirsh J, Miesenbock G
634 (2009) Writing memories with light-addressable reinforcement circuitry. Cell
635 139:405-415.

636 Clark JE, Naughton P, Shurey S, Green CJ, Johnson TR, Mann BE, Foresti R, Motterlini
637 R (2003) Cardioprotective actions by a water-soluble carbon
638 monoxide-releasing molecule. Circ Res 93:e2-8.

639 Cohn R, Morantte I, Ruta V (2015) Coordinated and Compartmentalized
640 Neuromodulation Shapes Sensory Processing in Drosophila. Cell
641 163:1742-1755.

642 Cui L, Yoshioka Y, Suyari O, Kohno Y, Zhang X, Adachi Y, Ikehara S, Yoshida T,
643 Yamaguchi M, Taketani S (2008) Relevant expression of Drosophila heme
644 oxygenase is necessary for the normal development of insect tissues.
645 Biochemical and biophysical research communications 377:1156-1161.

646 Cypionka H, Meyer O (1983) Carbon monoxide-insensitive respiratory chain of
647 Pseudomonas carboxydovorans. J Bacteriol 156:1178-1187.

648 Daniels RW, Gelfand MV, Collins CA, DiAntonio A (2008) Visualizing glutamatergic
649 cell bodies and synapses in Drosophila larval and adult CNS. J Comp Neurol
650 508:131-152.

651 Davis RL (2011) Traces of Drosophila memory. Neuron 70:8-19.

652 Diao F, Ironfield H, Luan H, Diao F, Shropshire WC, Ewer J, Marr E, Potter CJ,
653 Landgraf M, White BH (2015) Plug-and-play genetic access to drosophila cell
654 types using exchangeable exon cassettes. Cell Rep 10:1410-1421.

655 Dubnau J, Grady L, Kitamoto T, Tully T (2001) Disruption of neurotransmission in
656 Drosophila mushroom body blocks retrieval but not acquisition of memory.
657 Nature 411:476-480.

658 Dura JM, Preat T, Tully T (1993) Identification of linotte, a new gene affecting learning
659 and memory in Drosophila melanogaster. J Neurogenet 9:1-14.

660 Durante W, Christodoulides N, Cheng K, Peyton KJ, Sunahara RK, Schafer AI (1997)
661 cAMP induces heme oxygenase-1 gene expression and carbon monoxide
662 production in vascular smooth muscle. Am J Physiol 273:H317-323.

663 Endo M (2009) Calcium-induced calcium release in skeletal muscle. Physiol Rev
664 89:1153-1176.

665 Friggi-Grelin F, Coulom H, Meller M, Gomez D, Hirsh J, Birman S (2003) Targeted
666 gene expression in Drosophila dopaminergic cells using regulatory sequences
667 from tyrosine hydroxylase. J Neurobiol 54:618-627.

668 Gerber B, Tanimoto H, Heisenberg M (2004) An engram found? Evaluating the
669 evidence from fruit flies. Curr Opin Neurobiol 14:737-744.

670 Giannini G, Conti A, Mammarella S, Scrobogna M, Sorrentino V (1995) The ryanodine
671 receptor/calcium channel genes are widely and differentially expressed in
672 murine brain and peripheral tissues. J Cell Biol 128:893-904.

673 Goncharenko K, Eftekharpour E, Velumian AA, Carlen PL, Fehlings MG (2014)
674 Changes in gap junction expression and function following ischemic injury of
675 spinal cord white matter. Journal of neurophysiology 112:2067-2075.

676 Gu H, O'Dowd DK (2007) Whole cell recordings from brain of adult Drosophila. J Vis
677 Exp:248.

678 Gubernator NG, Zhang H, Staal RG, Mosharov EV, Pereira DB, Yue M, Balsanek V,
679 Vadola PA, Mukherjee B, Edwards RH, Sulzer D, Sames D (2009) Fluorescent
680 false neurotransmitters visualize dopamine release from individual presynaptic
681 terminals. Science 324:1441-1444.

682 Hanbauer I, Wink D, Osawa Y, Edelman GM, Gally JA (1992) Role of nitric oxide in
683 NMDA-evoked release of [3H]-dopamine from striatal slices. Neuroreport
684 3:409-412.

685 Hiramatsu M, Yokoyama S, Nabeshima T, Kameyama T (1994) Changes in
686 concentrations of dopamine, serotonin, and their metabolites induced by carbon
687 monoxide (CO) in the rat striatum as determined by in vivo microdialysis.
688 Pharmacol Biochem Behav 48:9-15.

689 Horiuchi J (2019) Recurrent loops: Incorporating prediction error and semantic/episodic
690 theories into Drosophila associative memory models. Genes Brain
691 Behav:e12567.

692 Huang G, Chen S, Li S, Cha J, Long C, Li L, He Q, Liu Y (2007) Protein kinase A and
693 casein kinases mediate sequential phosphorylation events in the circadian
694 negative feedback loop. Genes Dev 21:3283-3295.

695 Huang YY, Kandel ER (1995) D1/D5 receptor agonists induce a protein
696 synthesis-dependent late potentiation in the CA1 region of the hippocampus.
697 Proc Natl Acad Sci U S A 92:2446-2450.

698 Ichinose T, Aso Y, Yamagata N, Abe A, Rubin GM, Tanimoto H (2015) Reward signal
699 in a recurrent circuit drives appetitive long-term memory formation. Elife
700 4:e10719.

701 Iliadi KG, Avivi A, Iliadi NN, Knight D, Korol AB, Nevo E, Taylor P, Moran MF,
702 Kamyshev NG, Boulianne GL (2008) nemy encodes a cytochrome b561 that is
703 required for Drosophila learning and memory. Proc Natl Acad Sci U S A
704 105:19986-19991.

705 Jacobitz S, Meyer O (1989) Removal of CO dehydrogenase from Pseudomonas
706 carboxydovorans cytoplasmic membranes, rebinding of CO dehydrogenase to
707 depleted membranes, and restoration of respiratory activities. J Bacteriol
708 171:6294-6299.

709 Jay TM (2003) Dopamine: a potential substrate for synaptic plasticity and memory
710 mechanisms. Progress in neurobiology 69:375-390.

711 Kakizawa S (2013) Nitric Oxide-Induced Calcium Release: Activation of Type 1
712 Ryanodine Receptor, a Calcium Release Channel, through Non-Enzymatic

713 Post-Translational Modification by Nitric Oxide. Front Endocrinol (Lausanne)
714 4:142.

715 Kakizawa S, Yamazawa T, Chen Y, Ito A, Murayama T, Oyamada H, Kurebayashi N,
716 Sato O, Watanabe M, Mori N, Oguchi K, Sakurai T, Takeshima H, Saito N, Iino
717 M (2012) Nitric oxide-induced calcium release via ryanodine receptors regulates
718 neuronal function. EMBO J 31:417-428.

719 Katz B, Miledi R (1967) Ionic requirements of synaptic transmitter release. Nature
720 215:651.

721 Kay AR, Alfonso A, Alford S, Cline HT, Holgado AM, Sakmann B, Snitsarev VA,
722 Stricker TP, Takahashi M, Wu LG (1999) Imaging synaptic activity in intact
723 brain and slices with FM1-43 in C. elegans, lamprey, and rat. Neuron
724 24:809-817.

725 Kijima Y, Ogunbunmi E, Fleischer S (1991) Drug action of thapsigargin on the Ca2+
726 pump protein of sarcoplasmic reticulum. J Biol Chem 266:22912-22918.

727 Kitagishi H, Negi S, Kiriyama A, Honbo A, Sugiura Y, Kawaguchi AT, Kano K (2010)
728 A diatomic molecule receptor that removes CO in a living organism. Angew
729 Chem Int Ed Engl 49:1312-1315.

730 Kitamoto T (2001) Conditional modification of behavior in Drosophila by targeted
731 expression of a temperature-sensitive shibire allele in defined neurons. J
732 Neurobiol 47:81-92.

733 Korshunova TA, Balaban PM (2014) Nitric oxide is necessary for long-term facilitation
734 of synaptic responses and for development of context memory in terrestrial
735 snails. Neuroscience 266:127-135.

736 Lanner JT, Georgiou DK, Joshi AD, Hamilton SL (2010) Ryanodine receptors: structure,
737 expression, molecular details, and function in calcium release. Cold Spring Harb
738 Perspect Biol 2:a003996.

739 Lee JH, Lee S, Kim JH (2016) Amygdala Circuits for Fear Memory: A Key Role for

740 Dopamine Regulation. Neuroscientist.

741 Liu C, Kershberg L, Wang J, Schneeberger S, Kaeser PS (2018) Dopamine Secretion Is
742 Mediated by Sparse Active Zone-like Release Sites. Cell 172:706-718 e715.

743 Liu C, Placais PY, Yamagata N, Pfeiffer BD, Aso Y, Friedrich AB, Siwanowicz I, Rubin
744 GM, Preat T, Tanimoto H (2012) A subset of dopamine neurons signals reward
745 for odour memory in Drosophila. Nature 488:512-516.

746 Lonart G, Cassels KL, Johnson KM (1993) Nitric oxide induces calcium-dependent
747 [3H]dopamine release from striatal slices. J Neurosci Res 35:192-198.

748 Lu YF, Hawkins RD (2002) Ryanodine receptors contribute to cGMP-induced
749 late-phase LTP and CREB phosphorylation in the hippocampus. Journal of
750 neurophysiology 88:1270-1278.

751 Mao Z, Davis RL (2009) Eight different types of dopaminergic neurons innervate the
752 Drosophila mushroom body neuropil: anatomical and physiological
753 heterogeneity. Frontiers in neural circuits 3:5.

754 Mao Z, Roman G, Zong L, Davis RL (2004) Pharmacogenetic rescue in time and space
755 of the rutabaga memory impairment by using Gene-Switch. Proc Natl Acad Sci
756 U S A 101:198-203.

757 Marin EC, Jefferis GS, Komiyama T, Zhu H, Luo L (2002) Representation of the
758 glomerular olfactory map in the Drosophila brain. Cell 109:243-255.

759 Maruyama T, Kanaji T, Nakade S, Kanno T, Mikoshiba K (1997) 2APB,
760 2-aminoethoxydiphenyl borate, a membrane-penetrable modulator of
761 Ins(1,4,5)P3-induced Ca2+ release. Journal of biochemistry 122:498-505.

762 Matsuda W, Furuta T, Nakamura KC, Hioki H, Fujiyama F, Arai R, Kaneko T (2009)
763 Single nigrostriatal dopaminergic neurons form widely spread and highly dense
764 axonal arborizations in the neostriatum. The Journal of neuroscience : the
765 official journal of the Society for Neuroscience 29:444-453.

766 McGuire SE, Le PT, Davis RL (2001) The role of Drosophila mushroom body signaling

767 in olfactory memory. Science 293:1330-1333.

768 McGuire SE, Le PT, Osborn AJ, Matsumoto K, Davis RL (2003) Spatiotemporal rescue
769 of memory dysfunction in Drosophila. Science 302:1765-1768.

770 Meinrenken CJ, Borst JG, Sakmann B (2003) Local routes revisited: the space and time
771 dependence of the Ca2+ signal for phasic transmitter release at the rat calyx of
772 Held. The Journal of physiology 547:665-689.

773 Michel BW, Lippert AR, Chang CJ (2012) A reaction-based fluorescent probe for
774 selective imaging of carbon monoxide in living cells using a palladium-mediated
775 carbonylation. J Am Chem Soc 134:15668-15671.

776 Miesenbock G, De Angelis DA, Rothman JE (1998) Visualizing secretion and synaptic
777 transmission with pH-sensitive green fluorescent proteins. Nature 394:192-195.

778 Miyashita T, Oda Y, Horiuchi J, Yin JC, Morimoto T, Saitoe M (2012) Mg(2+) block of
779 Drosophila NMDA receptors is required for long-term memory formation and
780 CREB-dependent gene expression. Neuron 74:887-898.

781 Molina-Luna K, Pekanovic A, Rohrich S, Hertler B, Schubring-Giese M, Rioult-Pedotti
782 MS, Luft AR (2009) Dopamine in motor cortex is necessary for skill learning
783 and synaptic plasticity. PLoS One 4:e7082.

784 Muller U (1994) Ca2+/calmodulin-dependent nitric oxide synthase in Apis mellifera
785 and Drosophila melanogaster. The European journal of neuroscience
786 6:1362-1370.

787 Muller U (1996) Inhibition of nitric oxide synthase impairs a distinct form of long-term
788 memory in the honeybee, Apis mellifera. Neuron 16:541-549.

789 Ng M, Roorda RD, Lima SQ, Zemelman BV, Morcillo P, Miesenbock G (2002)
790 Transmission of olfactory information between three populations of neurons in
791 the antennal lobe of the fly. Neuron 36:463-474.

792 Oyamada T, Hayashi T, Kagaya A, Yokota N, Yamawaki S (1998) Effect of dantrolene
793 on K(+)- and caffeine-induced dopamine release in rat striatum assessed by in

794 vivo microdialysis. Neurochem Int 32:171-176.

795 Park SY, Kim JH, Lee SJ, Kim Y (2013) Involvement of PKA and HO-1 signaling in
796 anti-inflammatory effects of surfactin in BV-2 microglial cells. Toxicol Appl
797 Pharmacol 268:68-78.

798 Pereira DB, Schmitz Y, Meszaros J, Merchant P, Hu G, Li S, Henke A, Lizardi-Ortiz JE,
799 Karpowicz RJ, Jr., Morgenstern TJ, Sonders MS, Kanter E, Rodriguez PC,
800 Mosharov EV, Sames D, Sulzer D (2016) Fluorescent false neurotransmitter
801 reveals functionally silent dopamine vesicle clusters in the striatum. Nature
802 neuroscience 19:578-586.

803 Pfeiffer BD, Truman JW, Rubin GM (2012) Using translational enhancers to increase
804 transgene expression in Drosophila. Proc Natl Acad Sci U S A 109:6626-6631.

805 Poss KD, Thomas MJ, Ebralidze AK, O'Dell TJ, Tonegawa S (1995) Hippocampal
806 long-term potentiation is normal in heme oxygenase-2 mutant mice. Neuron
807 15:867-873.

808 Puig MV, Antzoulatos EG, Miller EK (2014) Prefrontal dopamine in associative
809 learning and memory. Neuroscience 282:217-229.

810 Regehr WG, Carey MR, Best AR (2009) Activity-dependent regulation of synapses by
811 retrograde messengers. Neuron 63:154-170.

812 Regulski M, Tully T (1995) Molecular and biochemical characterization of dNOS: a
813 Drosophila Ca2+/calmodulin-dependent nitric oxide synthase. Proc Natl Acad
814 Sci U S A 92:9072-9076.

815 Rice ME, Cragg SJ (2008) Dopamine spillover after quantal release: rethinking
816 dopamine transmission in the nigrostriatal pathway. Brain Res Rev 58:303-313.

817 Rorig B, Klausa G, Sutor B (1996) Intracellular acidification reduced gap junction
818 coupling between immature rat neocortical pyramidal neurones. The Journal of
819 physiology 490 (Pt 1):31-49.

820 Sabatini BL, Regehr WG (1996) Timing of neurotransmission at fast synapses in the

mammalian brain. Nature 384:170-172.

Sacca GB, Saenz DA, Jaliffa CO, Minces L, Keller Sarmiento MI, Rosenstein RE (2003) Photic regulation of heme oxygenase activity in the golden hamster retina: involvement of dopamine. Journal of neurochemistry 85:534-542.

Sagara Y, Inesi G (1991) Inhibition of the sarcoplasmic reticulum Ca2+ transport ATPase by thapsigargin at subnanomolar concentrations. J Biol Chem 266:13503-13506.

Shibuki K, Kimura S, Wakatsuki H (2001) Suppression of the induction of long-term depression by carbon monoxide in rat cerebellar slices. The European journal of neuroscience 13:609-616.

Stewart BA, Atwood HL, Renger JJ, Wang J, Wu CF (1994) Improved stability of Drosophila larval neuromuscular preparations in haemolymph-like physiological solutions. J Comp Physiol A 175:179-191.

Stone JR, Marletta MA (1994) Soluble guanylate cyclase from bovine lung: activation with nitric oxide and carbon monoxide and spectral characterization of the ferrous and ferric states. Biochemistry 33:5636-5640.

Sugimura Y, Yoshizaki F, Katagiri J, Horiuchi C (1980) Studies on algal cytochromes. I. Purification and properties of cytochrome b-561 from Enteromorpha prolifera. Journal of biochemistry 87:541-547.

Sun F et al. (2018) A Genetically Encoded Fluorescent Sensor Enables Rapid and Specific Detection of Dopamine in Flies, Fish, and Mice. Cell 174:481-496 e419.

Takasago T, Imagawa T, Furukawa K, Ogurusu T, Shigekawa M (1991) Regulation of the cardiac ryanodine receptor by protein kinase-dependent phosphorylation. Journal of biochemistry 109:163-170.

Takemura SY et al. (2017) A connectome of a learning and memory center in the adult Drosophila brain. Elife 6.

Tamura T, Chiang AS, Ito N, Liu HP, Horiuchi J, Tully T, Saitoe M (2003) Aging specifically impairs amnesiac-dependent memory in Drosophila. Neuron 40:1003-1011.

Taskiran D, Kutay FZ, Pogun S (2003) Effect of carbon monoxide on dopamine and glutamate uptake and cGMP levels in rat brain. Neuropsychopharmacology : official publication of the American College of Neuropsychopharmacology 28:1176-1181.

Tinajero-Trejo M, Denby KJ, Sedelnikova SE, Hassoubah SA, Mann BE, Poole RK (2014) Carbon monoxide-releasing molecule-3 (CORM-3; Ru(CO)3Cl(glycinate)) as a tool to study the concerted effects of carbon monoxide and nitric oxide on bacterial flavohemoglobin Hmp: applications and pitfalls. J Biol Chem 289:29471-29482.

Tully T, Quinn WG (1985) Classical conditioning and retention in normal and mutant Drosophila melanogaster. J Comp Physiol A 157:263-277.

Ueno K, Naganos S, Hirano Y, Horiuchi J, Saitoe M (2013) Long-term enhancement of synaptic transmission between antennal lobe and mushroom body in cultured Drosophila brain. The Journal of physiology 591:287-302.

Ueno K, Suzuki E, Naganos S, Ofusa K, Horiuchi J, Saitoe M (2017) Coincident postsynaptic activity gates presynaptic dopamine release to induce plasticity in Drosophila mushroom bodies. Elife 6.

Verkhratsky A (2005) Physiology and pathophysiology of the calcium store in the endoplasmic reticulum of neurons. Physiol Rev 85:201-279.

Vreman HJ, Ekstrand BC, Stevenson DK (1993) Selection of metalloporphyrin heme oxygenase inhibitors based on potency and photoreactivity. Pediatric research 33:195-200.

Wan K, Moriya T, Akiyama M, Takeshima H, Shibata S (1999) Involvement of ryanodine receptor type 3 in dopamine release from the striatum: evidence from mutant mice lacking this receptor. Biochemical and biophysical research

876 communications 266:588-592.

877 Wang R, Wu L (2003) Interaction of selective amino acid residues of K(ca) channels
878 with carbon monoxide. Exp Biol Med (Maywood) 228:474-480.

879 Wang Y, Wu J, Rowan MJ, Anwyl R (1996) Ryanodine produces a low frequency
880 stimulation-induced NMDA receptor-independent long-term potentiation in the
881 rat dentate gyrus in vitro. The Journal of physiology 495 (Pt 3):755-767.

882 Wang Y, Mamiya A, Chiang AS, Zhong Y (2008) Imaging of an early memory trace in
883 the Drosophila mushroom body. The Journal of neuroscience : the official
884 journal of the Society for Neuroscience 28:4368-4376.

885 Wong AM, Wang JW, Axel R (2002) Spatial representation of the glomerular map in the
886 Drosophila protocerebrum. Cell 109:229-241.

887 Xu L, Eu JP, Meissner G, Stamler JS (1998) Activation of the cardiac calcium release
888 channel (ryanodine receptor) by poly-S-nitrosylation. Science 279:234-237.

889 Yagishita S, Hayashi-Takagi A, Ellis-Davies GC, Urakubo H, Ishii S, Kasai H (2014) A
890 critical time window for dopamine actions on the structural plasticity of
891 dendritic spines. Science 345:1616-1620.

892 Yamasaki M, Takeuchi T (2017) Locus Coeruleus and Dopamine-Dependent Memory
893 Consolidation. Neural Plast 2017:8602690.

894 Yu D, Akalal DB, Davis RL (2006) Drosophila alpha/beta mushroom body neurons
895 form a branch-specific, long-term cellular memory trace after spaced olfactory
896 conditioning. Neuron 52:845-855.

897 Zalk R, Lehnart SE, Marks AR (2007) Modulation of the ryanodine receptor and
898 intracellular calcium. Annu Rev Biochem 76:367-385.

899 Zhao F, Li P, Chen SR, Louis CF, Fruen BR (2001) Dantrolene inhibition of ryanodine
900 receptor Ca2+ release channels. Molecular mechanism and isoform selectivity. J
901 Biol Chem 276:13810-13816.

902 Zhu XZ, Luo LG (1992) Effect of nitroprusside (nitric oxide) on endogenous dopamine
903 release from rat striatal slices. Journal of neurochemistry 59:932-935.

904 Zhuo M, Small SA, Kandel ER, Hawkins RD (1993) Nitric oxide and carbon monoxide
905 produce activity-dependent long-term synaptic enhancement in hippocampus.
906 Science 260:1946-1950.

907 Zorzato F, Scutari E, Tegazzin V, Clementi E, Treves S (1993) Chlorocresol: an
908 activator of ryanodine receptor-mediated Ca2+ release. Mol Pharmacol
909 44:1192-1201.

910

Figures and legends

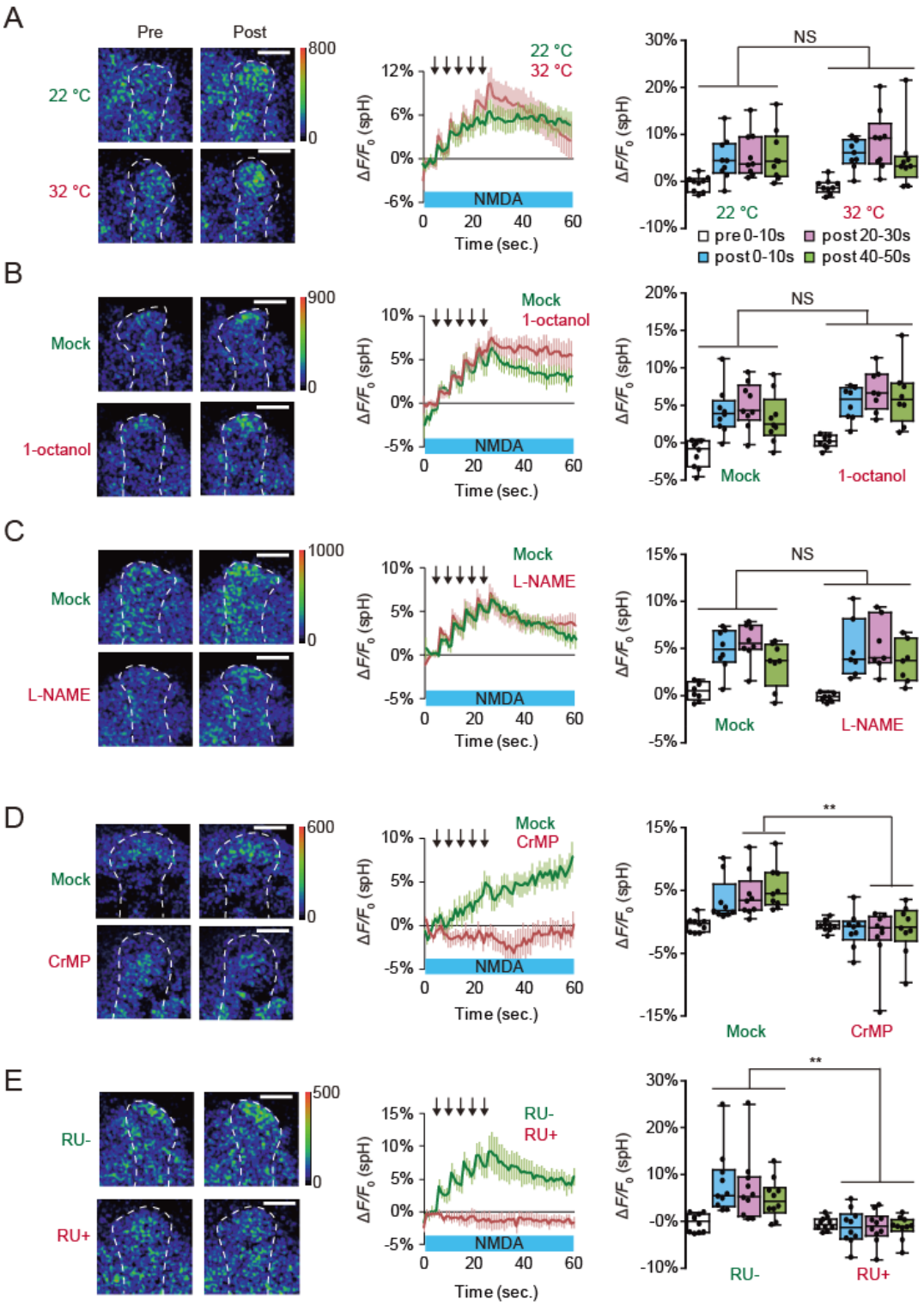

Fig. 1. Inhibiting heme oxygenase (HO) activity in the MBs blocks SV exocytosis

from pre-synaptic DA terminals

A, Blocking SV exocytosis from the MBs does not affect DA release. spH fluorescence was measured at TH-DA terminals innervating the α3/α'3 compartments of the MB vertical lobes in *MB-LexA>LexAop-shi^{ts}* brains. (Left) typical pseudocolor images 5 s before and 30 s after coincident AL + NMDA activation. (Middle) time course of fluorescent changes, and (right) summary graphs. Two-way ANOVA indicates no significant differences in spH fluorescence between restrictive (32 °C) and permissive (22 °C) temperatures. N = 9 for all data. Scale bars = 20 μm. **B**, The gap junction inhibitor, 1-octanol, does not affect DA release. Two-way ANOVA indicates no significant differences in spH fluorescence between mock and 1-octanol conditions. N = 8 for all data. **C,** The NOS inhibitor, L-NAME, does not affect SV exocytosis from TH-DA terminals. Two-way ANOVA indicates no significant differences in spH fluorescence due to drug treatment. N=8 for all data. **D,** The HO inhibitor, CrMP, prevents DA release. Two-way ANOVA indicates significant differences in spH fluorescence due to drug treatment ($F_{3, 64}$ = 3.268, P = 0.0268, N = 9 for mock and N = 10 for 10 μM CrMP). * P < 0.05 and ** P < 0.01 by Bonferroni *post hoc* tests. **E**, *dHO* knockdown in the MBs prevents DA release. Two-way ANOVA indicates significant differences in spH fluorescence due to RU treatment ($F_{3, 72}$ = 4.265, P = 0.0079, N = 10 for all data). ** P < 0.01 by Bonferroni *post hoc* tests.

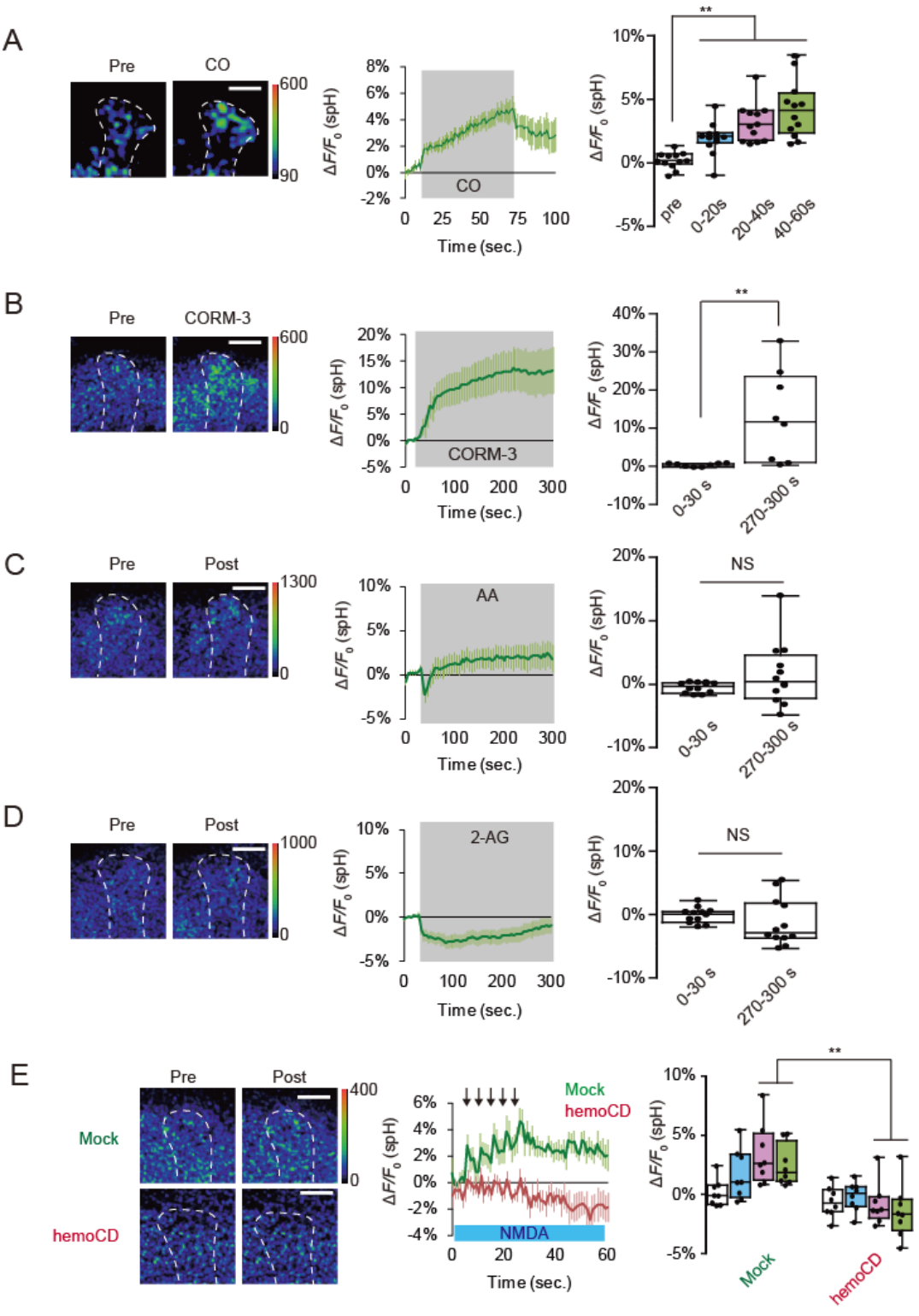

933

934 **Fig. 2. CO evokes SV exocytosis from DA terminals**

935 **A**, CO induces DA release. CO-saturated saline was puffed onto the vertical lobes of the
936 MB during the indicated time period (gray-shaded area in the middle panel).
937 CO-induced spH responses were obtained by subtracting spH fluorescent changes
938 induced by control N_2-satulated saline from fluorescence changes induced by
939 CO-saturated saline. One-way ANOVA and post hoc tests indicate significant changes
940 in spH fluorescence upon CO application ($F_{3,44}$= 14.994, P < 0.001). N = 12 for all data.
941 **B**, CORM-3 induces DA release. 20 μM CORM-3 (dissolved in 0.2% DMSO) was bath
942 applied and spH fluorescence was measured at DA terminals at the tip of the MB
943 vertical lobes. CORM-3-induced spH responses were obtained by subtracting
944 fluorescent changes induced by control 0.2% DMSO saline from fluorescence changes
945 induced by CORM-3. ** P < 0.01 determined by Student's t-test, comparing spH
946 responses before (0-30s) and after application of CO (270-300s). N = 8 for all data. **C**,
947 Arachidonic acid (AA) does not induce DA release. 200 μM AA (dissolved in 0.4 %
948 ethanol) was bath applied. AA-induced spH responses were obtained by subtracting
949 fluorescence changes induced by 0.4% ethanol saline from fluorescence changes
950 induced by AA. NS P > 0.05 by Mann Whitney test and N = 16 for all data. **D,** Effects
951 of 2-arachidonylglycerol (2-AG) on DA release. Bath application of 200 μM AG
952 (dissolved in 0.2 % DMSO) did not induce SV exocytosis in TH-DA terminals.
953 AG-induced spH responses were obtained by subtracting fluorescence changes induced
954 by 0.2% DMSO saline from fluorescence changes induced by AG. NS P > 0.05
955 determined by Student's t-test. N = 12 for all data. **E,** The CO scavenger, hemoCD,
956 prevents SV exocytosis from DA terminals. AL + NMDA-dependent changes in spH
957 fluorescence were measured in the presence and absence of 50 μM hemoCD. Two-way
958 ANOVA indicates significant decreases in spH fluorescence due to hemoCD treatment

($F_{3, 56}$ = 2.845, P = 0.0458, N = 8 for all data). ** P < 0.01 by Bonferroni *post hoc* tests.

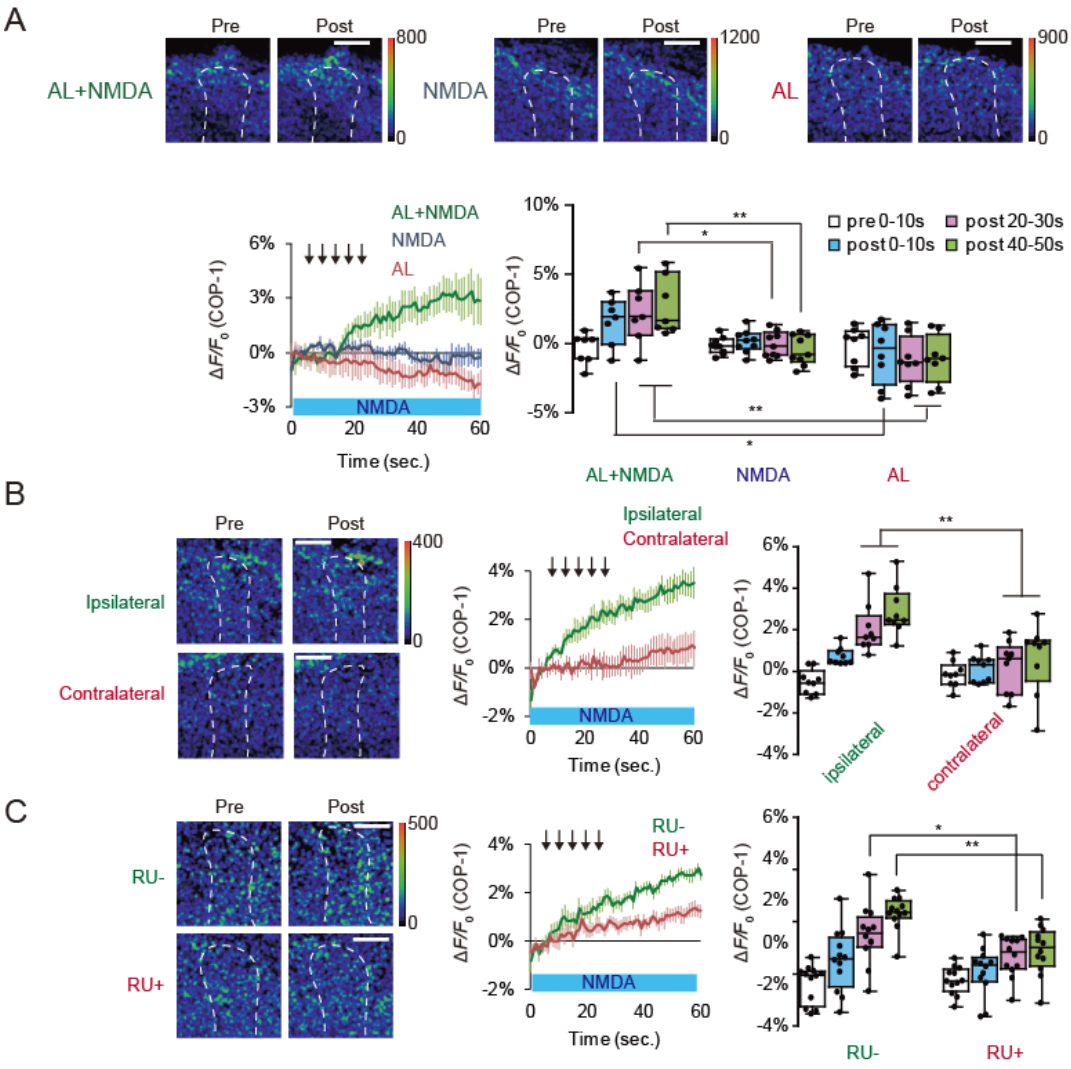

Fig. 3. Endogenous CO released from MBs induces DA release

A, Top panels, typical images of COP-1 fluorescence observed at the α3/α'3 compartments of the MB vertical lobes. Pre refers to images taken prior to stimulation, while Post refers to images taken 30 secs after onset of indicated stimuli. Lower left, time course of COP-1 fluorescence upon indicated stimulation protocols, and lower right, summary of COP-1 fluorescence at different time intervals upon indicated

968 stimulation. Isolated brains were incubated in 4 μM COP-1, and COP-1 responses were
969 calculated by subtracting non-stimulated fluorescence changes from stimulated
970 fluorescence changes. Two-way ANOVA indicates significant differences in COP-1
971 fluorescence due to treatment, time, and interaction between treatment and time ($F_{6, 84}$ =
972 3.094, P = 0.0087, N = 8 for AL or NMDA stimulation alone and N = 7 for AL +
973 NMDA stimulation). * P < 0.05 and ** P < 0.01 by Bonferroni *post hoc* tests. Scale
974 bars = 20 μm. **B,** CO is released from the MB lobe ipsilateral to AL stimulation.
975 Two-way ANOVA indicates significant differences in fluorescence between MB lobes
976 ($F_{3, 64}$ = 5.491, P = 0.020, N = 9 for all data). ** P < 0.01 by Bonferroni *post hoc* tests.
977 **C,** Knocking down *dHO* expression in the MBs impairs CO production. Two-way
978 ANOVA indicates significant differences in COP-1 fluorescence due to RU treatment
979 ($F_{3, 88}$ = 6.25, P = 0.0086, N = 12 for all data). ** P < 0.01 by Bonferroni *post hoc* tests.

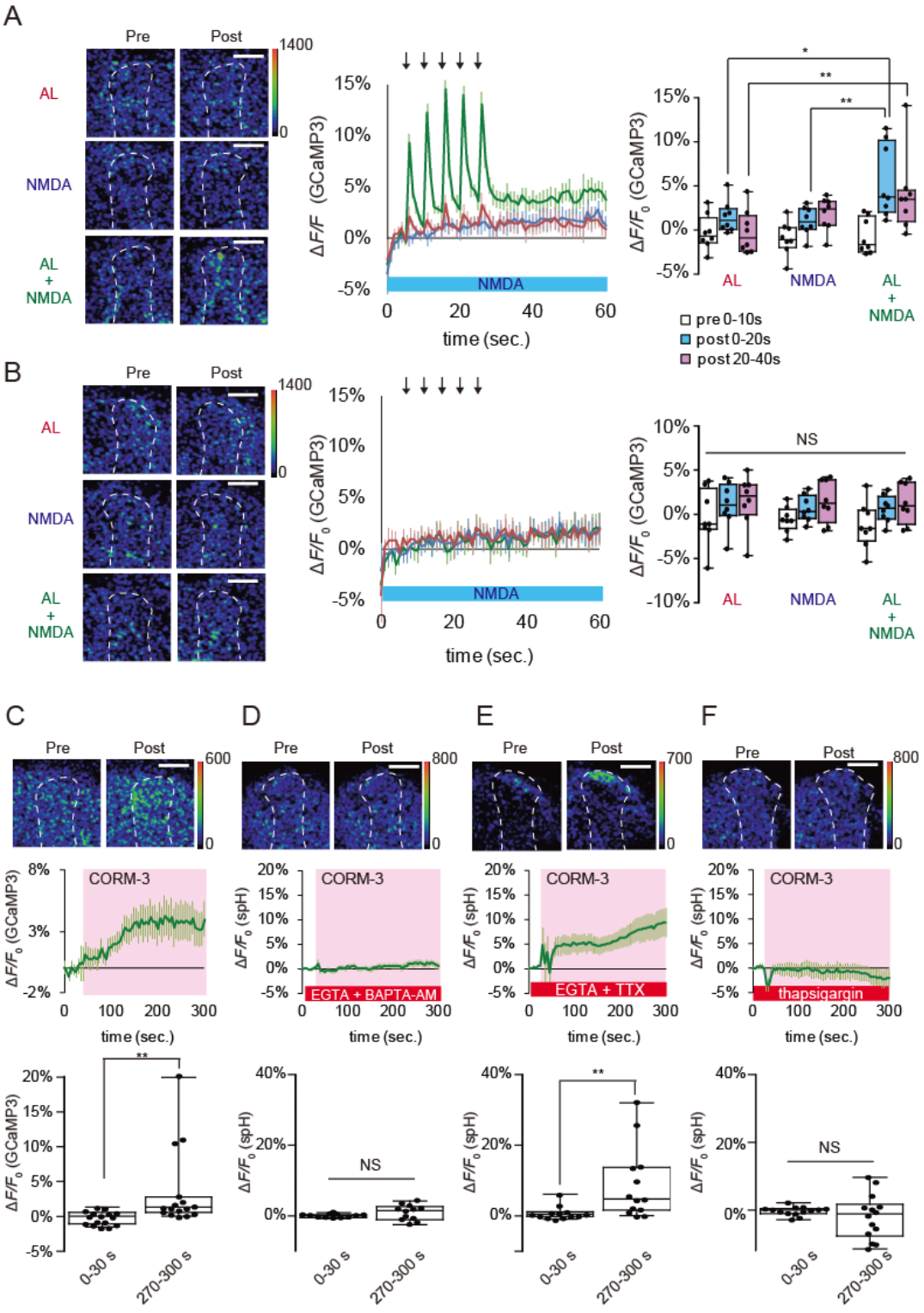

980

981 **Fig. 4. CO induced DA release requires Ca^{2+} efflux from internal Ca^{2+} stores.**

A, Left panel, typical pseudo color images of G-CaMP3 fluorescence in TH-DA terminals innervating the α3/α'3 compartments of the vertical MB lobes ipsilateral to AL stimulation. The type of stimulation applied is indicated on the left, and responses before (pre) and after (post) stimulation are shown. Middle panel, time course of Ca^{2+} responses in TH-DA terminals upon indicated stimulation. Right panel, summary of responses. Two-way ANOVA indicates significant differences in G-CaMP3 fluorescence due to stimulation type, time, and interaction between stimulation type and time ($F_{4, 63}$ = 2.610, P = 0.0437, N = 8 for all data). * $P < 0.05$ and ** $P < 0.01$ by Bonferroni *post hoc* tests. **B**, G-CaMP3 fluorescence changes in TH-DA terminals innervating the MB contralateral to AL stimulation. Panels are similar to those shown in (A). Two-way ANOVA indicates no significant differences in G-CaMP3 fluorescence due to time or stimulation type. N = 9 for all data. **C**, CORM-3 induces Ca^{2+} increases in TH-DA terminals. CORM-3 induced Ca^{2+} changes were calculated by subtracting fluorescence changes under mock conditions from changes induced by CORM-3. 20 μM CORM-3 (dissolved in 0.2% DMSO saline) was puffed onto the α3/α'3 compartments of the vertical MB lobes during the indicated time period (shown in pink in the middle panel). **$P < 0.01$ by Mann Whitney test. N = 16 for all data. **D**, CORM-3-induced DA release depends on increases in intracellular Ca^{2+}. Brains were incubated in Ca^{2+}-free external solution containing 2 mM EGTA and 10 μM BAPTA-AM for 10 min prior to CORM-3 application. P = 0.166 by Student's t-test. N = 12. **E**, CORM-3-induced DA release does not require influx of external Ca^{2+} or activity of voltage-gated Na^{+} channels. Brains were placed in Ca^{2+}-free external solution containing 5 mM EGTA and 10 μM TTX 10 min prior to CORM-3 application. **$P < 0.01$ by Mann Whitney test. N = 13. **F**, CORM-3-induced DA release requires efflux from internal Ca^{2+} stores. Brains were

1006 incubated in Ca^{2+}-free external solution containing 10 μM thapsigargin for 10 min prior

1007 to CORM-3 application. P = 0.364 by Student's t-test. N = 14.

1008

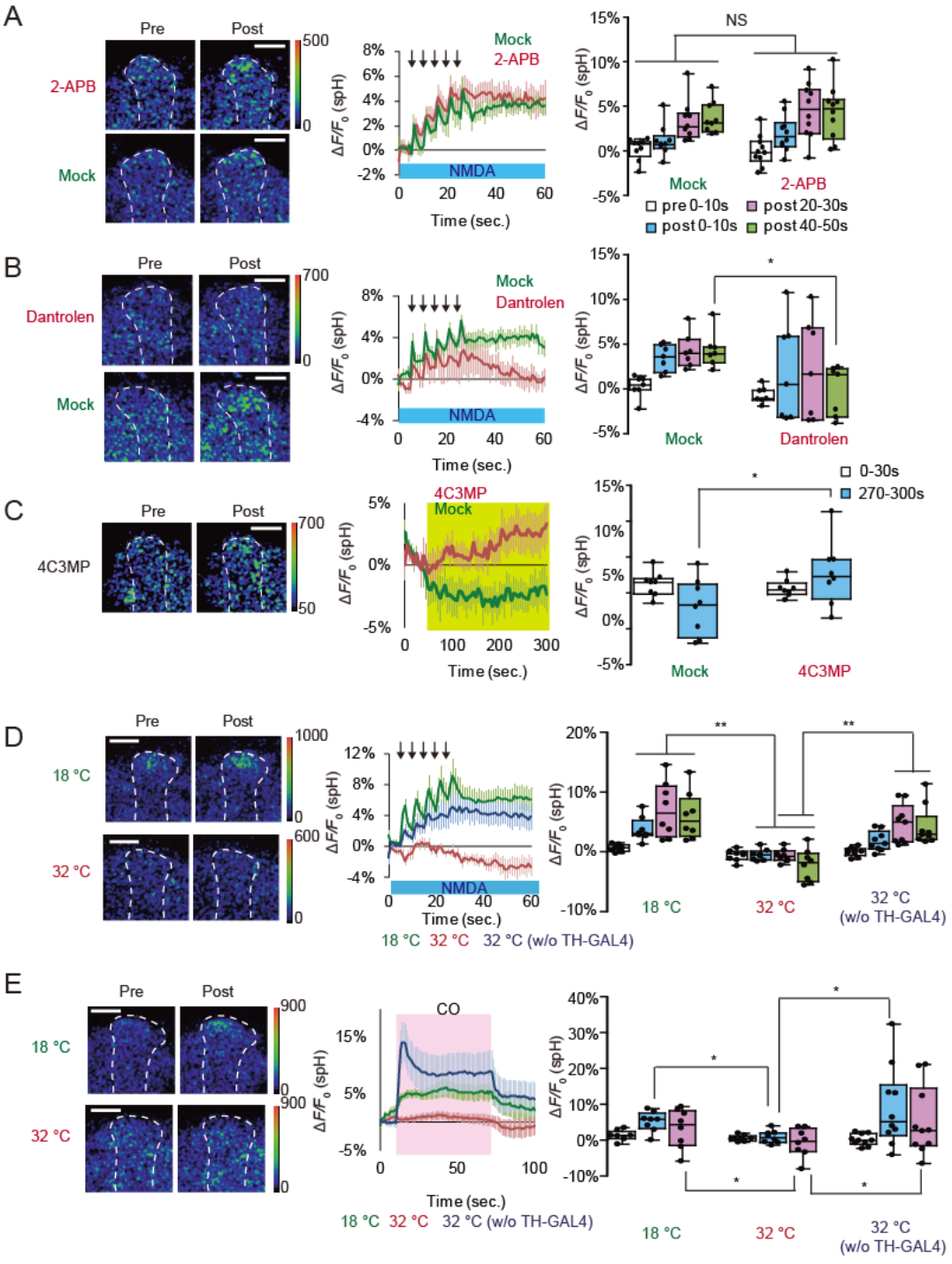

1009

Fig. 5. CO induced DA release is mediated by ryanodine receptors.

A, An IP_3R inhibitor does not affect DA release. 100 μM 2-aminoethoxydiphenylborane (2-APB) was dissolved in 0.1 % DMSO saline. Two-way ANOVA indicates no significant differences in spH fluorescence due to 2-APB treatment. N = 10 for 2-APB treatment and N = 9 for mock control. **B**, The RyR inhibitor, dantrolen, inhibits DA release. 10 μM dantrolen was dissolved in 0.1% DMSO saline. Two-way ANOVA indicates significant effects of drug treatment on spH fluorescence ($F_{1, 48}$ = 6.781, P = 0.0122, N = 8 for all data). *P < 0.05 compared with mock treated samples assayed by Bonferroni *post hoc* tests. **C**, Application of a RyR agonist induces DA release. 1 mM 4-chloro-3-methylphenol (4C3MP) was dissolved in 0.2% ethanol saline containing 1 μM TTX and applied for the indicated period of time (shown in yellow). ** P < 0.001 as assayed by Student's t-test comparing before (0-30 s) and after (280-300 s) 4C3MP treatment. N = 8 for all data. **D**, Temporal *RyR* knockdown at 30 °C in TH-DA neurons prevents DA release evoked by AL + NMDA stimulation. Two-way ANOVA indicates signifincant differences in spH fluorescence between restrictive and permissive temperatures ($F_{3,56}$ = 6.625, P = 0.0007, N = 8 for all data). ** P < 0.01 by Bonferroni *post hoc* tests. **E**, Temporal knock down of *RyR* in TH-DA neurons prevents DA release evoked by CO application. CO saturated saline was applied during the indicated time period (shown in pink) from a micropipet. Two-way ANOVA indicates significant interaction differences in spH fluorescence due to time, temperature, and interaction between time and temperature ($F_{2,42}$ = 12.6, P < 0.0001, N = 8 for all data). ** P < 0.01 by Bonferroni *post hoc* tests.

SUPPLEMENTAL INFROMATION FOR

"Carbon monoxide, a retrograde messenger generated in post-synaptic mushroom body neurons evokes non-canonical dopamine release."

Kohei Ueno[1]*, Johannes Morstein[2,3], Kyoko Ofusa[1], Shintaro Naganos[1], Ema Suzuki-Sawano[1], Saika Minegishi[4], Samir P. Rezgui[5], Hiroaki Kitagishi[4], Brian W. Michel[5], Christopher J. Chang[2], Junjiro Horiuchi[1], Minoru Saitoe[1]*

[1]Tokyo Metropolitan Institute of Medical Science, 2-1-6 Kamikitazawa, Setagaya-ku, Tokyo, 1568506, Japan.

[2]Departments of Chemistry and Howard Hughes Medical Institute, University of California, Berkeley.

[3]Department of Chemistry, New York University.

[4]Department of Molecular Chemistry and Biochemistry, Faculty of Science and Engineering, Doshisha University, Kyotanabe, Kyoto 610-0321, Japan.

[5]Department of Chemistry and Biochemistry, University of Denver.

*Correspondence to: Kohei Ueno (ueno-kh@igakuken.or.jp), and Minoru Saitoe (saito-mn@igakuken.or.jp)

THIS SUPPLEMENTAL INFROMATION INCLUDES:

Figures S1 to S4

Table S1

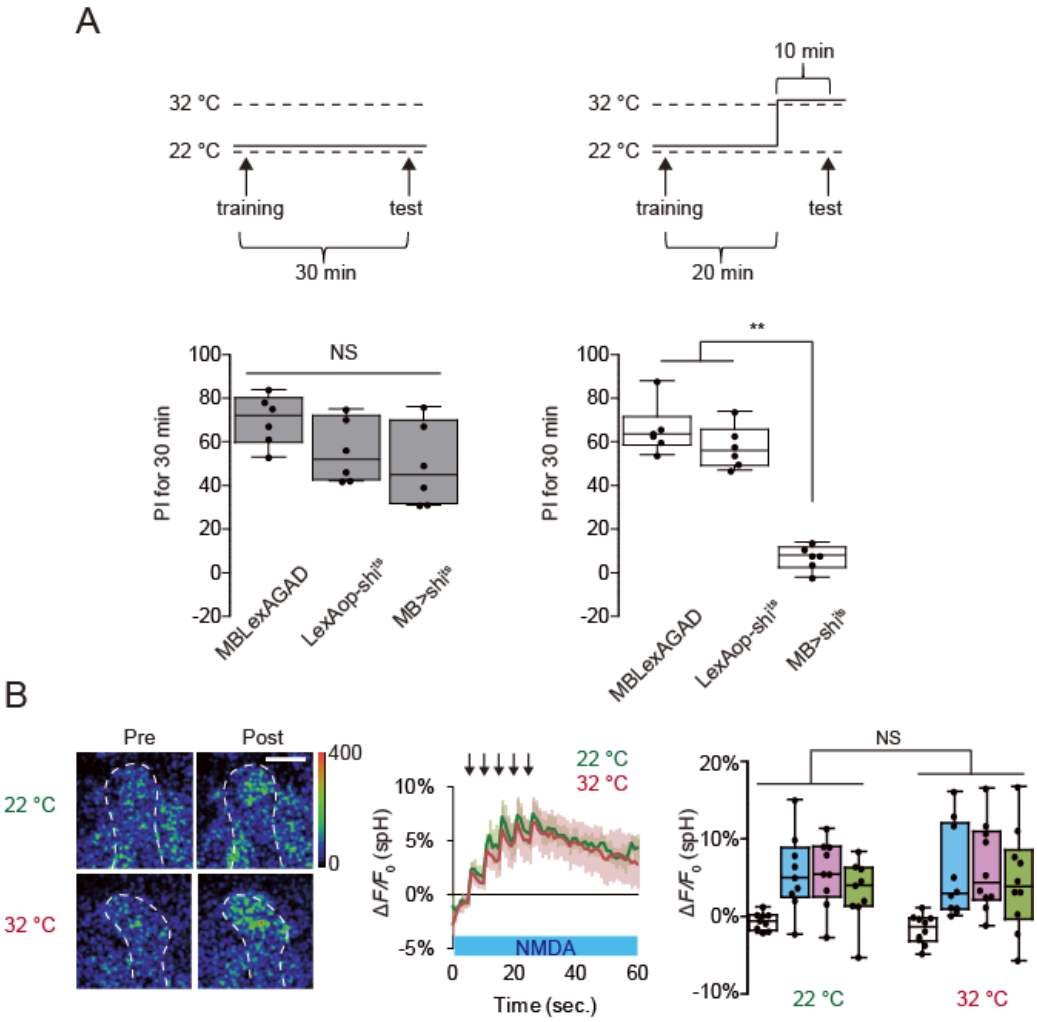

Figure S1 Coincident MB stimulation induces SV exocytosis from DA neurons. MB output is not required for DA release.

A, Inhibiting MB output impairs recall of olfactory memory. One-way ANOVA and Bonferroni post hoc tests indicate significant impairment in memory recall in *MB > shi^{ts}* flies at restrictive temperature (32°C) ($F_{2,15}$ = 71.05, P< 0.001) but not at permissive temperature (22°C) ($F_{2,15}$ = 2.854, P = *2.854*). **P < 0.01 and NS P > 0.05. N = 6 for all data. **B**, Inhibiting MB output did not affect DA release. Two-way ANOVA identified no significant changes in spH fluorescence between restrictive (32 °C) and permissive temperatures (22 °C). N = 9 for 32 °C and N = 10 for 22°C.

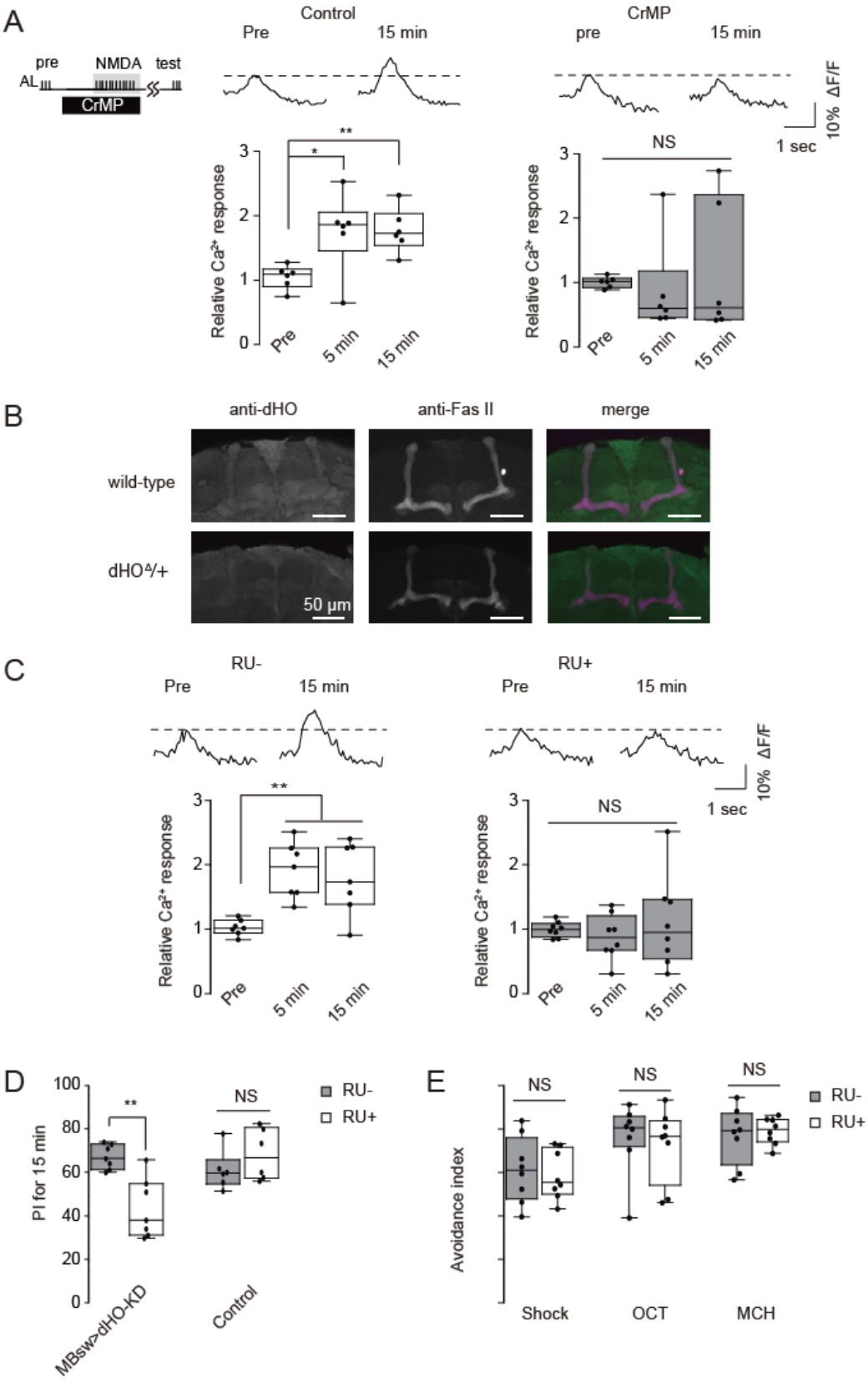

1067

Figure S2 dHO in the MBs is required LTE and olfactory learning.

A, Effects of HO inhibitor, CrMP, on LTE induced by AL+ NMDA stimulation. One-way ANOVA and Bonferroni post hoc tests indicate significant changes in AL-evoked Ca^{2+} responses in the MB after AL + NMDA stimulation in control conditions ($F_{2,15}$ = 5.836, P = 0.013, N = 6) and but not in 10 μM CrMP treated conditions ($F_{2,18}$ = 0.339, P = 0.717, N = 7). **B**, dHO antibody labels the MB lobes and midline cells in the *Drosophila* brain. Fas II antibody staining is included to identify subsets of the MB lobes. dHO signals are reduced in dHO^{Δ} hemizygotes (dHO^{Δ}/+) demonstrating the specificity of the antibody. **C**, Knockdown of *dHO* in the MBs impairs LTE induced by AL + NMDA stimulation. One-way ANOVA and Bonferroni post hoc tests indicate significant LTE in the MB after AL + NMDA stimulation in control (RU-) conditions where *dHO* is not knocked down (Left panel, $F_{2,18}$= 9.630, P = 0.001, N =7). LTE is not observed when dHO is knocked down (RU+) (Right panel, $F_{2,21}$= 0.444, P = 0.647, N = 8). **D**, Knocking down *dHO* in the MBs impairs olfactory learning. $^{**}P < 0.01$ determined by Student's t-test. N = 7 for all data. **e**, Naïve responses to odors and electrical shock are not affected by knocking down *dHO* in the MBs. N = 8 for all experiments.

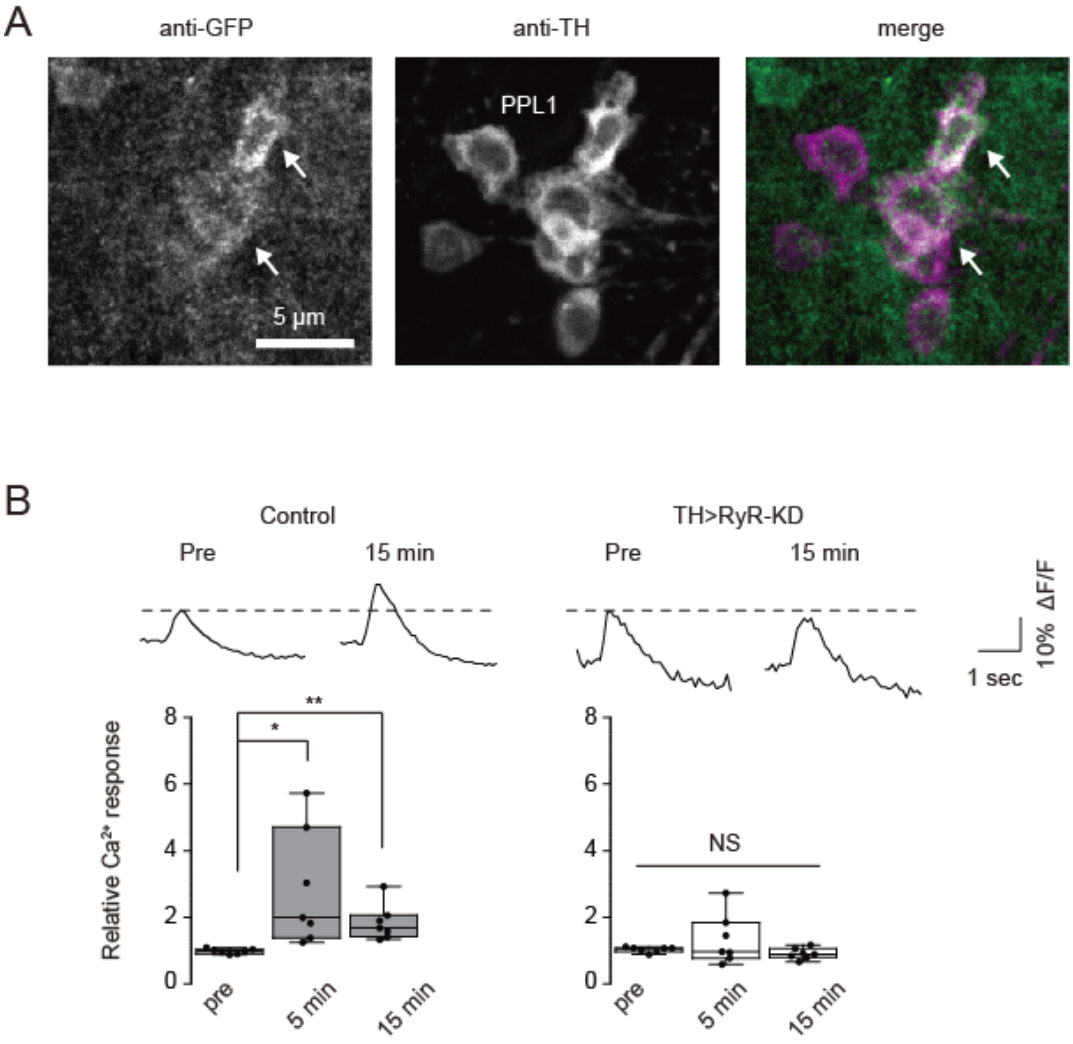

Figure S3 RyRs in TH-DA terminals are required for LTE.

A, RyR localization was examined in *UAS-mCD8::GFP/Mi{Trojan-GAL4.0} RyR[MI08146-TG4.0]* flies in which expression of mCD8::GFP is driven by Trojan-GAL4 inserted in the endogenous *RyR* gene. GFP expression overlapped with expression of tyrosine hydroxylase (TH) in PPL1 DA neurons (arrows) that innervate the vertical lobes of the MBs. **B**, Knocking down RyRs in TH-DA neurons abolishes LTE induced by AL + NMDA stimulation. One-way ANOVA and Bonferroni post hoc tests indicate significant increases in AL-evoked Ca^{2+} responses after AL + NMDA

stimulation in control brains ($F_{2,18}$= 5.455, P = 0.014) but not in TH>RyR-KD brains ($F_{2,18}$= 1.666, P = 0.217). N = 7 for all data.

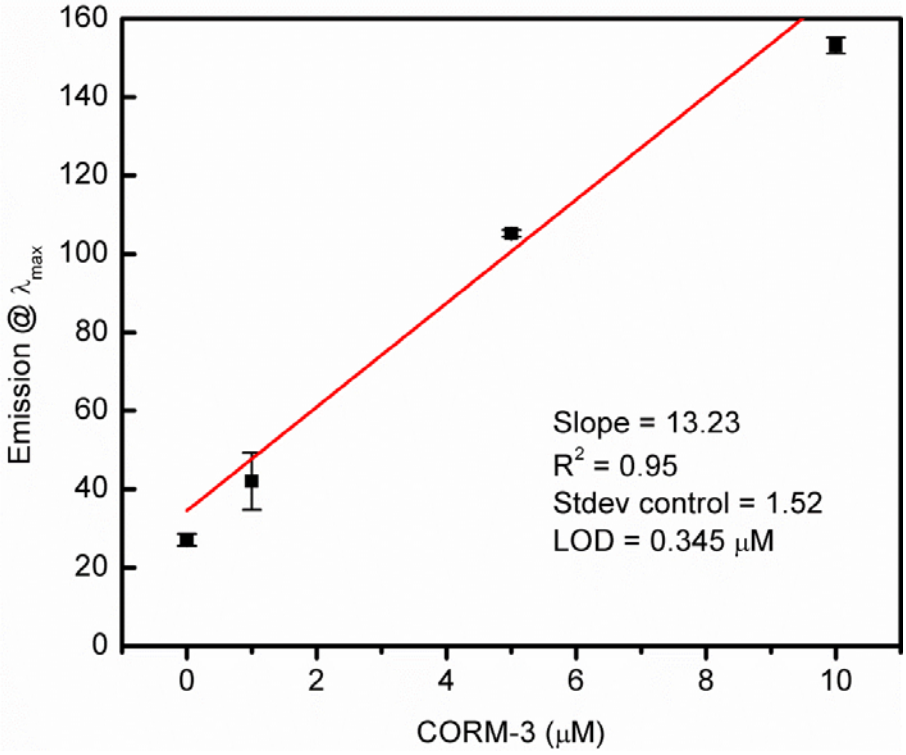

Figure S4 Limit of detection determination for COP-1.

Limit of detection (LOD) of COP-1 at 90 min determined by fluorescence intensity at 508 nm as a function of CORM-3 concentration. While LOD of COP-1 is 0.345 μM at 90 min, a similar range of LOD's were found at other timepoints (LOD = 0.660 μM at t = 30 min, 0.673 μM at t = 45 min, 0.556 μM at 60 min). Each concentration was run in triplicate and control was run five times. All data are shown as mean ± SD.

Table S1 Genotypes used in each experiment

Fig. #	genotype
1A	*UAS-spH/MB-LexA:GAD;TH-GAL4/LexAop-shi^{ts}*
1B	*UAS-spH; TH-GAL4*
1C	*UAS-spH; TH-GAL4*
1D	*UAS-spH; TH-GAL4*
1E	*UAS-dicer/LexAop-spH;UAS-dHO-IR, MBsw/TH-LexAGAD*
2A	*UAS-spH; TH-GAL4*
2B	*UAS-spH; TH-GAL4*
2C	*UAS-spH; TH-GAL4*
2D	*UAS-spH; TH-GAL4*
3A	*MB-LexA:GAD, LexAop-R-GECO1*
3B	*MB-LexA:GAD, LexAop-R-GECO1*
3C	*MB-LexA:GAD, LexAop-R-GECO1/UAS-dicer; UAS-dHOIR, MBsw*
3D	*MB-LexA:GAD, LexAop-R-GECO1/UAS-spH; TH-GAL4*
4A	*MB-LexA:GAD, LexAop-R-GECO1/UAS-G-CaMP3; TH-GAL4*
4B	*MB-LexA:GAD, LexAop-R-GECO1/UAS-G-CaMP3; TH-GAL4*
4C	*UAS-G-CaMP3; TH-GAL4*
4D	*UAS-spH; TH-GAL4*
4E	*UAS-spH; TH-GAL4*
4F	*UAS-spH; TH-GAL4*
5A	*UAS-spH; TH-GAL4*
5B	*UAS-spH; TH-GAL4*
5C	*UAS-spH; TH-GAL4*
5D	*UAS-RyR RNAi, tubp-GAL80(ts)/LexAop-spH; TH-GAL4/TH-LexAp65*
5E	*UAS-RyR RNAi, tubp-GAL80(ts)/LexAop-spH; TH-GAL4/TH-LexAp65*

Supplementary Fig. #	
S1A	*UAS-spH; TH-GAL4*
S1B	*MB-LexA:GAD, LexAop-G-CaMP2*
S1C	*MB-LexA:GAD, LexAop-G-CaMP2*

S2A	*MB-LexA:GAD; LexAop-shi^{ts} as MB > shi^{ts}*
	MB-LexA:GAD
	LexAop-shi^{ts}
S2B	*c747-GAL4/LexAop-spH;UAS-shi^{ts}/TH-LexAp65*
S3A	*MB-LexA:GAD, LexAop-G-CaMP2*
S3B	*CS(w) as wild-type*
	Df(3R)Exel7309/+ as dHO$^{\Delta}$/+
S3C	*UAS-dicer/MBLexA:GAD, LexAop-G-CaMP2;UAS-dHO-IR, MBsw/+*
S3D	*UAS-dicer/+; MBsw, UAS-dHO-IR/Df(3R)Exel7309* as *MBsw > UAS-dHO IR*
	UAS-dicer/+; Df(3R)Exel7309/+ as control
S4A	*Mi{Trojan-GAL4.0}RyR[MI08146-TG4.0]/UAS-mCD8::GFP*
S4B	*UAS-G-CaMP2/+; TH-GAL4 as control*
	UAS-RyR RNAi/UAS-G-CaMP2/+; TH-GAL4 as TH>RyR-KD

1108